Science of the Total Environment 754 (2021) 142312

Contents lists available at ScienceDirect

Science of the Total Environment

journal homepage: www.elsevier.com/locate/scitotenv

Natural attenuation of lead by microbial manganese oxides in a karst aquifer

Laura Newsome [a,*], Charles G.D. Bacon [b], Hokyung Song [a], Yunyao Luo [a], David M. Sherman [b], Jonathan R. Lloyd [a]

[a] Williamson Research Centre, Department of Earth and Environmental Sciences, University of Manchester, Manchester M13 9PL, United Kingdom
[b] School of Earth Sciences, University of Bristol, Wills Memorial Building, Queens Road, Bristol BS8 1RJ, United Kingdom

HIGHLIGHTS

- Pb is a toxic environmental contaminant and is present at many mining sites.
- Mn(IV)-oxide minerals have a strong affinity for metals, including Pb.
- Birnessite cave crusts were associated with Mn(II)-oxidising microbial communities.
- Bacteria were isolated that could oxidise Mn(II) in the presence of Pb.
- Microbial Mn(II)-oxidation proposed to sequester Pb from contaminated waters.

GRAPHICAL ABSTRACT

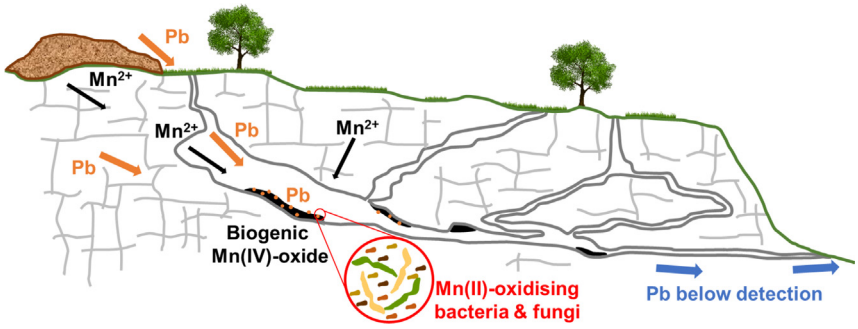

ARTICLE INFO

Article history:
Received 17 July 2020
Received in revised form 7 September 2020
Accepted 7 September 2020
Available online 21 September 2020

Editor: Frederic Coulon

Keywords:
Bioremediation
Natural analogue
Birnessite
Fungi
Bacteria
Microbial community

ABSTRACT

Lead is a toxic environmental contaminant associated with current and historic mine sites. Here we studied the natural attenuation of Pb in a limestone cave system that receives drainage from the ancient Priddy Mineries, UK. Extensive deposits of manganese oxides were observed to be forming on the cave walls and as coatings in the stream beds. Analysis of these deposits identified them as birnessite (δ-MnO_2), with some extremely high concentrations of sorbed Pb (up to 56 wt%) also present. We hypothesised that these cave crusts were actively being formed by microbial Mn(II)-oxidation, and to investigate this the microbial communities were characterised by DNA sequencing, enrichment and isolation experiments. The birnessite deposits contained abundant and diverse prokaryotes and fungi, with ~5% of prokaryotes and ~ 10% of fungi closely related to known heterotrophic Mn(II)-oxidisers. A substantial proportion (up to 17%) of prokaryote sequences were assigned to groups known as autotrophic ammonia and nitrite oxidisers, suggesting that nitrogen cycling may play an important role in contributing energy and carbon to the cave crust microbial communities and consequently the formation of Mn(IV) oxides and Pb attenuation. Enrichment and isolation experiments showed that the birnessite deposits contained Mn(II)-oxidising microorganisms, and two isolates (*Streptomyces* sp. and *Phyllobacterium* sp.) could oxidise Mn(II) in the presence of 0.1 mM Pb. Supplying the enrichment cultures with acetate as a source of energy and carbon stimulated Mn(II)-oxidation, but excess organics in the form of glucose generated aqueous Mn(II), likely via microbial Mn(IV)-reduction. In this karst cave, microbial Mn(II)-oxidation contributes to the active sequestration and natural attenuation of Pb from contaminated waters, and therefore may be considered a natural analogue for the design of wastewater remediation systems and for understanding the geochemical controls on karst groundwater quality, a resource relied upon by billions of people across the globe.

* Corresponding author at: Camborne School of Mines and Environment and Sustainability Institute, University of Exeter, Penryn, Cornwall TR10 9FE, United Kingdom.
E-mail address: l.newsome@exeter.ac.uk (L. Newsome).

https://doi.org/10.1016/j.scitotenv.2020.142312

1. Introduction

Lead is a common environmental contaminant, toxic to humans affecting all organs, and a designated mutagen, teratogen, and probable carcinogen. Pb exposure is thought to cause to >1 million deaths per year, contribute to the risk of mental disorders, and even low levels of exposure may cause irreversible effects on child intellectual development (O'Connor et al., 2020; Stanaway et al., 2018; World Health Organisation, 2010). Significant Pb contamination is present in the Priddy area of the Mendip Hills, Somerset, UK, where galena (PbS) was mined and processed from pre-Roman times up until the early 20th century (British Geological Survey, 2017). Reported concentrations of Pb in soils in the vicinity of the St Cuthbert's Leadworks, Priddy, range from 0.18 to 172 g kg^{-1} (Allison, 2002). Major cave systems underlie the former Leadworks including the St Cuthbert's Swallet, which is known to have been impacted by Pb contamination from as early as 1863 (British Geological Survey, 2017). The area has now been designated as the 'Priddy Mineries Nature Reserve', with distinctive habitats, rich wetland flora, and rare species that thrive on the Pb-rich soils (British Geological Survey, 2017).

Cave systems provide unique habitats for microbial life and metabolisms (Summers Engel, 2015), as well as an opportunity to study subsurface processes. The St Cuthbert's Swallet is a 7 km long deep phreatic cave system developed in steeply dipping Carboniferous limestone deposits (Irwin, 1991; Waltham et al., 1997). Manganese oxide cave crusts have been discovered within the cave system (Bacon, 2014). Mn(IV) oxide minerals can often be found in caves, with many studies proposing that microbial activity was responsible for their formation (Northup and Lavoie, 2001; Rossi et al., 2010). Indeed it has been suggested that most naturally-occurring Mn(IV) oxides are likely to be of biogenic origin (Tebo et al., 2014, 2004). The oxidation of Mn(II) has a high activation energy, but the reaction can be catalysed by microbial activity leading to biological Mn(II)-oxidation occurring up to five orders of magnitude faster than abiotic oxidation or surface catalysed oxidation (Tebo, 1991), although at pH values >9, abiotic Mn(II) oxidation becomes more favourable (Nealson, 2006). Key to the formation of biogenic Mn(IV) oxide deposits is a continuous supply of Mn(II), which commonly occurs at redox interfaces.

Microbial Mn(II)-oxidation can occur directly via Mn oxidases (heme peroxidases or multicopper oxidases) (Anderson et al., 2009; Romano et al., 2017; Webb et al., 2005), and/or indirectly via superoxide formation (Hansel et al., 2012; Learman et al., 2011; Tebo et al., 2005). Both processes involve the transfer of a single electron to Mn(II), forming Mn(III) which can be stabilised by ligands and siderophores, or disproportionate to Mn(II) and Mn(IV) (Duckworth and Sposito, 2005; Geszvain et al., 2012; Tebo et al., 2004). Almost all known Mn (II)-oxidising microbes are heterotrophs (Tebo et al., 2005), but the first report of a chemolithoautotrophic Mn(II)-oxidiser in 2020 demonstrated that a bacterium assigned to the Nitrospirae is able to conserve energy from extracellular Mn(II)-oxidation coupled to aerobic respiration, and autotrophic C fixation from CO_2 (Yu and Leadbetter, 2020). Mn(II)-oxidising microbes are ubiquitous in the environment and are phylogenetically diverse, including prokaryotes and fungi (Carmichael and Bräuer, 2015; Tebo et al., 2005). It has been proposed that intracellular Mn(II) acts as an antioxidant to protect cells from reactive oxygen species (Daly et al., 2004), while the formation of extracellular Mn(IV) oxides may benefit microbes by protecting them from environmental hazards, predation, phage infection or heavy metal toxicity (Tebo et al., 2005).

Interestingly, the St Cuthbert's Swallet cave system contains deposits that are significantly enriched in Pb (Stenner, 1979, 1978, 1977a). These deposits were suspected to be (Stenner, 1977b), and recently confirmed as Mn oxides (Bacon, 2014). Natural and synthetic Mn oxides are well known to have a strong affinity for heavy metals, especially Pb (Tebo et al., 2004). Natural Mn oxides are known to scavenge Pb from lake waters (Dong et al., 2003), soils (McKenzie, 1980), from the oceans into deep-sea ocean nodules (Sherman and Peacock, 2010) and in cave systems. Rossi et al. (2010) reported Mn oxides of biogenic origin in caves in northern Spain, where the Mn oxides had average concentrations of 10.4% Zn and 1.2% Pb (from the dissolution of the sphalerite-galena mineralization hosted by the local geology). Mn oxides have even been proposed as a means to treat Pb-contaminated wastewaters (Boujelben et al., 2009) and soils (McCann et al., 2015).

Pb exhibits toxic effects in microorganisms, it can bind to sulfhydryl, phosphate and hydroxyl functional groups, leading to the damage of DNA, proteins and cell membranes (Kushwaha et al., 2018; Roane et al., 2015; Van Der Heggen et al., 2010). The particularly high concentrations of Pb present in the St Cuthbert's Swallet deposits raises questions about whether they contain viable microbial communities that are capable of oxidising Mn(II). Metal-resistance mechanisms (including for Pb) are found in many microorganisms, such as using efflux pumps, binding to metallothionein-like proteins, siderophore production, and the precipitation of extracellular Pb minerals (Liang et al., 2016; Rensing et al., 1998; Schalk et al., 2011; Sharma et al., 2017). Pb toxicity has been linked to oxidative stress in experiments using *Saccharomyces cerevisiae*; Pb exposure was also shown to cause significant oxidative stress leading to apotosis, but adding a scavenger of the reactive oxygen species enhanced cell survival (Bussche and Soares, 2011). One of the reasons why microbes form Mn(IV) oxides is thought to be as a protective mechanism against oxidative stress (Tebo et al., 2005), therefore the substantial quantities of Mn(IV) oxides found in the St Cuthbert's Swallet may represent evidence of scavenging of the reactive oxygen species produced by the microbial community in response to the significant levels of Pb contamination. While some of the aforementioned studies included biogenic or natural Mn oxides, none considered the effect of Pb on microbial Mn(II)-oxidation. Exploration of this ecosystem could therefore offer insights into microbial functioning in metal-impacted Mn oxides, and their potential for application in metal remediation scenarios.

Here we aimed to investigate the hypothesis that microbial communities were present in these Pb-rich Mn(IV) oxide cave crusts, and were actively contributing to their formation via Mn(II)-biooxidation. The composition of the microbial community was characterised and a series of isolation and enrichment experiments performed, to understand more about the functions of this microbial ecosystem and associated biogeochemical interactions, in a unique subsurface environment. The cave crusts contained diverse and abundant microbial communities, with many sequences closely related to known Mn(II)-oxidising prokaryotes and fungi, and with isolates that were indeed able oxidise Mn(II) in the presence of Pb. Together this demonstrates how microbial activity can contribute to the natural attenuation of Pb contamination from historic mining activities.

2. Materials and methods

2.1. Sample collection

Samples of Mn-rich cave crusts were collected from St Cuthbert's Swallet (Mendip Hills, Priddy, Somerset, UK) by the Bristol Exploration Caving Club (*Table S1*). In September 2012, solid samples (cave pebbles from the floor of the cave) were collected from seven different locations, from the entrance down to the furthest point that is accessible (Sump 2), and placed separately into new plastic sample bags for mineralogical characterisation. Eight stream water samples from different positions (where the cavers were physically able to sample) along the main cave passage were also taken using dedicated disposable syringes. In April 2013, additional samples were collected by C.G.D.B from Wookey Hole Cave chambers at the resurgence of the cave stream at the foot of the Mendip Hills, approximately 4 km (as measured linearly on the Earth's surface) from the cave entrance at the top of the Mendip Hills. These comprised loose sediment and pool water, as well as pore water

which was collected from sediment in the laboratory by centrifugation (Eppendorf 5810, 20,900*g* 5 min).

Samples were collected for microbiological characterisation by the Bristol Exploration Caving Club in January 2017. These comprised six solid samples and six cave waters collected from three different locations within the St Cuthbert's Swallet cave (*Table S1*, *Fig. S1*). The samples were transferred into sterile containers and immediately shipped to the University of Manchester under ice. The samples were stored in a cold room in the dark at 10 °C to replicate the conditions in the UK subsurface.

2.2. Solid phase characterisation

The samples collected in September 2012 were subjected to a suite of analyses to determine the mineralogy of the cave crusts and the host phases of the metals. Scanning electron microscopy (SEM) was performed to collect electron backscatter images, using a Hitachi S-3500 N SEM equipped with an energy dispersive spectroscopy (EDS) detector for element quantification. Where possible, small cave pebbles were either attached to carbon pads on sample holders, or the powdered scrapes of crusts were set in epoxy resin and finely polished to expose the grains. EDS point analyses were made on randomly selected locations on each sample with a minimum target of 10 separate location analyses per sample where possible. EDS point analyses had acquisition times of 60 s. For routine EDS analysis, the detection limits are about 0.1 wt%. The high heterogeneity and diversity of these samples inherently limits the accuracy of the EDS quantifications. Furthermore, since no reference standard for this material is available to verify the analysis conditions, the accuracy of the analysis cannot be defined. As such the individual results should be treated as being semi-quantitative.

X-ray powder diffraction (XRD) and Raman spectroscopy was used to identify the mineral phases present in crustal material scraped from a cobble from St. Cuthbert's Sump II. The crust sample selected for XRD analysis was from the deepest sample location possible in the cave where all stream waters converge, and shown by EDS to have the greatest mass of Pb present. XRD was performed using a Philips Xpert Pro XRD diffractometer with a graphite monochromatized CuKα1 source ($k = 1.5406$ Å) (generator voltage of 40 keV; tube current of 30 mA). The spectra was acquired from 10 to 90° 2θ, at a 0.02° 2θ step size with 3 s (or 12 s) dwell time per step. Raman spectroscopy was performed using a Thermo Raman spectrometer, calibrated at 532 nm using a silicon wafer. The reference material of vernadite/birnessite (δ-MnO_2) was made following the method of Villalobos et al. (2003).

To further investigate the relationships between different elements, μ-X-ray fluorescence (μ-XRF) mapping was performed at the MicroXAS beamline station, at the Swiss Light Source (SLS). Selected samples from Wookey Hole Cave Chambers at the resurgence of St Cuthbert's Swallet, as well as sediment samples from the mines at the entrance to St Cuthbert's Swallet were mounted in epoxy resin and polished down to <100 μm thick films. Samples were mounted at 45° from the incident beam. The fluorescence detector was positioned at 10 cm, 90° from the incident beam. The beam size was 6 μm horizontal, 3 μm vertical. The energy used was 13.136 keV, 7th harmonic.

To confirm that the 2017 samples closely resembled the 2012/13 samples, aliquots of cave crusts A2 and B4 were dried, mounted on silicon wafers, and gold coated. SEM was performed using a Phillips XL30 ESEM-FEG operated in high vacuum conditions. Images were collected, and elemental proportions identified on three areas of each sample using EDS. In addition, total organic carbon (TOC) was measured on dried powdered cave crusts using a Shimadzu SSM5000A.

2.3. Aqueous geochemistry

For the 2012 cave stream waters, the samples were filtered (0.22 μm), acidified with 2% HNO_3, placed under ice and taken directly to the Earth Sciences laboratory in Bristol, then refrigerated and analysed within 48 h after sampling using ICP-OES (Agilent 710). Triplicate samples of cave waters were not logistically practical and because of the constant flow of the cave waters would have natural heterogeneity on short time scales. For analytical control, blank MilliQ water samples were analysed every three samples to check for cross contamination and analytical errors. Water quality results by ICP-OES are approximately $\pm$10 ppb.

To characterise the composition of the cave waters collected in 2017, aliquots were immediately filtered (0.45 μm), and the filtrate was analysed for major anions and volatile fatty acids by ion chromatography (Dionex ICS 5000), or acidified with 2% HNO_3 and analysed for metals by ICP-MS (Agilent 7500CX). The pH was measured on the unfiltered samples.

2.4. Microbial community characterisation

The 2017 samples were prepared for microbial community analysis. Immediately after arrival in the laboratory, around 0.25 g of material was removed from Samples A1, A2, B4 and B6 using a sterile spatula (*Table S1*, *Fig. S1*). Two of the three adjacent samples (A3 and C5) were rock samples and it was not possible to remove any surface material for analysis. DNA was extracted using a QIAGEN PowerSoil DNA extraction kit, amplified and visualised to identify the presence of prokaryotic and eukaryotic microbial communities. The prokaryotic DNA was amplified using the universal 16S rRNA amplicon primers 8F and 1492R (Lane, 1991), eukaryotic DNA using the EUKF and EUKR primers (Medlin et al., 1988) and fungal DNA using the Internal Transcribed Spacer region (ITS) primers ITS1F and ITS4 (Brown et al., 1993; Gardes and Bruns, 1993). The purity of the polymerase chain reaction (PCR) products was determined by visualisation under shortwave UV light after staining with Sybersafe® and separation by electrophoresis in Tris-acetate-EDTA gel. No bands were visible for Sample A1, indicating that it was unlikely to contain sufficient DNA for sequencing. The abundance of DNA was determined in Samples A2, B4 and B6 using quantitative PCR (see the *Supplementary Material* for details).

To characterise the prokaryotic community present in Samples A2, B4 and B6, the 16S rRNA amplicon was sequenced using the Illumina MiSeq platform (Illumina, San Diego, CA, USA) targeting the V4 hyper variable region (forward primer, 515F, 5′-GTGYCAGCMGCCGCGGTAA-3′; reverse primer, 806R, 5′-GGACTACHVGGGTWTCTAAT-3′) for 2 × 250-bp paired-end sequencing (Illumina) (Caporaso et al., 2012, 2011). PCR amplification was performed using Roche FastStart High Fidelity PCR System (Roche Diagnostics Ltd., Burgess Hill, UK) in 50 μL reactions under the following conditions: initial denaturation at 95 °C for 2 min, followed by 36 cycles of 95 °C for 30 s, 55 °C for 30 s, 72 °C for 1 min, and a final extension step of 5 min at 72 °C. The PCR products were purified and normalised to ~20 ng each using the SequalPrep Normalization Kit (Fisher Scientific, Loughborough, UK). The PCR amplicons from all samples were pooled in equimolar ratios. The run was performed using a 4 pM sample library spiked with 4 pM PhiX to a final concentration of 10% following the method of Schloss and Kozich (Kozich et al., 2013).

To characterise the fungal community present in Samples A2, B4 and B6, sequencing of PCR amplicons of the ITS2 region of nuclear ribosomal DNA was conducted with the Illumina MiSeq platform (Illumina, San Diego, CA, USA), targeting the ITS2 internal transcribed spacer region between the large subunit (LSU) and the 5.8S ribosomal genes (forward primer, ITS4F, 5′-AGCCTCCGCTTATTGATATGCTTAART-3′, reverse primer, 5.8SR, 5′-AACTTTYRRCAAYGGATCWCT-3′) (Taylor et al., 2016) for 2 × 300-bp paired-end sequencing (Illumina) (Caporaso et al., 2012, 2011). PCR amplification was performed using Roche FastStart High Fidelity PCR System (Roche Diagnostics Ltd., Burgess Hill, UK) in 50 μL reactions under the following conditions: initial denaturation at 95 °C for 2 min, followed by 36 cycles of 95 °C for 30 s, 56 °C for 45 s, 72 °C for 2 min, and a final extension step of 5 min at 72 °C. The PCR products were purified and normalised to ~20 ng each using the

SequalPrep Normalization Kit (Fisher Scientific, Loughborough, UK). The PCR amplicons from all samples were pooled in equimolar ratios. The run was performed using a 10 pM sample library spiked with 10 pM PhiX to a final concentration of 10% (Kozich et al., 2013).

16S rRNA gene and ITS amplicon sequence data were processed using QIIME2 software 2019.1 release (Bolyen et al., 2019) following the "Moving Pictures" tutorial (QIIME2docs, 2020). The DADA2 plug-in (Callahan et al., 2016) was used for quality control and amplicon sequence variance (ASV) assignment. The Silva database v. 132 (Quast et al., 2013) was used for the classification of bacterial 16S rRNA gene ASVs and the UNITE database v. 8.2 (Nilsson et al., 2019) was used for the classification of fungal ITS ASVs. For 16S rRNA datasets, ASVs classified as chloroplast or mitochondria were removed and for ITS datasets, ASVs classified as archaea, bacteria, or other non-fungal eukaryotes were removed. For further analysis, ASVs that were detected above 10 in negative controls were removed. Blastn was used to identify the closest GenBank matches (NCBI, 2020). For fungi, the ITS Reference Sequences search was used (NCBI, 2015).

Functional abundances were predicted based on 16S rRNA gene sequences using PICRUSt2 software v. 2.2.0 (Douglas et al., 2019) following the tutorial provided by the developer (Douglas, 2019). The relative abundance of predicted genes was calculated by dividing the abundance of each gene by the sum of all gene abundances per sample. There are limitations that should be considered with this approach. PICRUSt2 searches the query sequences through a reference genomic tree and uses the functional profile of the closest relatives (Douglas, 2020); the genomic profile of prokaryotes can vary even at strain level, while the 16S rRNA sequences have limited resolution. FUNGuild software v 1.0 (Nguyen et al., 2016) was used to obtain functional guild composition of ITS fungal data. Details of the command lines used are provided in the *Supplementary Material*.

2.5. Isolation and enrichment of Mn(II)-oxidising microorganisms

To investigate whether active Mn(II)-oxidising microorganisms were present within the metal-rich cave crusts, isolation experiments were performed using freshwater minimal medium (mM $NaHCO_3$ 30, NH_4Cl 4.7, KCl 1.3, $NaH_2PO_4 \cdot H_2O$ 4.3, yeast extract 0.1, HEPES 20, trace vitamins and minerals, after Lovley et al., 1991 and Tebo et al., 2014) agar plates at pH 7.0, with 10 mM acetate or 10 mM glucose as the carbon source and 1 mM $MnCl_2$ as the source of Mn(II). The cave crust Sample A2 was selected for use in the isolation experiments due to its higher Mn content, and because more colonies formed in preliminary tests. Aliquots were suspended in sterile deionised water and used to inoculate the plates, which were incubated in the dark at 20 °C. Control plates were not inoculated to identify the occurrence of any abiotic Mn(II)-oxidation. The formation of Mn(IV) oxides was identified using leucoberbelin blue (LBB) dye (Tebo et al., 2014).

After observing the growth of fungi on the plates but not the presence of Mn(IV) oxides, a 1% Nystatin solution (0.02 g Nystatin in 4 mL DMSO) was added to the freshwater minimal medium plates to inhibit fungal growth. Subsequently the growth of brown colonies was observed which tested positive for Mn(IV) oxides using the LBB dye; these isolates were sub-cultured and maintained on freshwater minimal medium plates. To investigate whether the isolates could grow, and oxidise Mn(II) in the presence of high concentrations of lead, 0.1 mM (21 mg L^{-1}) of Pb as $PbCl_2$ was added to freshwater minimal medium agar plates, with acetate or glucose as the carbon source and with and without 1 mM $MnCl_2$ as the source of Mn(II).

The isolates were visualised using SEM and optical microscopy. Colonies were mobilised by adding around 20 μL of sterile deionised water to the plates, and then dropped onto glass slides for optical microscopy, or for SEM onto silicon wafers, air dried and gold coated. SEM was performed using a Phillips XL30 ESEM-FEG operated in high vacuum conditions. Secondary electron (SE) and backscatter secondary electron (BSE) images were collected. The presence of Mn minerals was identified using an EDAX Genesis EDS system. Sanger sequencing was used to identify the isolates (see the *Supplementary Material* for details).

Experiments were performed to enrich for Mn(II)-oxidising microorganisms and monitor the associated geochemical changes. Four aliquots of the cave crusts (0.15 g) were diluted into 15 mL of filter-sterilised deionised water, shaken, and 0.3 mL of this suspension was used to inoculate 30 mL of freshwater minimal medium, as described above but omitting the agar, in 250 mL Erlenmeyer flasks closed with a foam bung and capped with Al foil. The flasks were stored at room temperature on an orbital shaker (110 rpm). Initial tests showed that Mn(II) was removed from solution within 3 days in the experiments and controls, primarily due to the formation of Mn(II)-carbonate and Mn(II)–phosphate minerals (precipitates identified via X-ray diffraction, Bruker D8 Advance) rather than abiotic oxidation. To avoid this effect, the freshwater medium was modified by replacing the HEPES buffer with MOPS (23 mM), omitting the $NaHCO_3$ and lowering the concentration of $NaH_2PO_4.2H_2O$ from 4.3 mM to 0.43 mM. Again, 10 mM acetate (as CH_3COONa, 20 mM C) or 10 mM glucose (as D-glucose $C_6H_{12}O_6$, 60 mM C) were supplied as the carbon source and 0.1–0.15 mM $MnCl_2$ was added as the source of Mn(II). Aqueous Mn(II) in enrichment media was determined by the formaldoxime colorimetric assay (Tebo et al., 2014). A calibration curve was made with known $MnSO_4 \cdot H_2O$ standards from 0 to 5 ppm, and selected results were confirmed with ICP-AES (Perkin-Elmer Optima 5300 DV).

3. Results and discussion

3.1. Geochemistry and mineralogy of the cave crust samples

Electron microscopy showed that the cave crusts had rough, irregular, amorphous botryoidal textures, high surface areas, and concentric growth patterns in cross sections (Fig. 1). The convex-outward microlamination and stromatolite-like textures are consistent with ferromanganese formations observed in other cave systems around the world, and are suggestive of a biogenic origin (Carpenter et al., 1978; Carpenter and Hayes, 1980; Gázquez et al., 2012, 2011; Rossi et al., 2010; White et al., 2009).

SEM and EDS analysis of cave crusts from a wide selection of sample locations in the St Cuthbert's Swallet cave system confirmed that these crusts were composed predominantly of an amorphous Mn phase with major enrichment of heavy metals, most notably Pb (up to 55.8 wt%) (*Table S2*).

The EDS analysis revealed that the Pb and Zn in these crusts were distributed throughout the concentric layers of cave crusts and present across the wide range of the sample locations. Covariant plots of Pb and Zn against Fe and Mn showed that for most samples there was a fairly strong positive correlation (R^2 0.46–0.76) between Pb and Mn (Fig. 2A), but not particularly with Fe (*Fig. S2*). The EDS analysis also revealed a highly varied stoichiometry of Pb/Zn and Mn, and some samples contained little Pb or Zn relative to Mn.

μ-XRF mapping results confirmed the strong relationship between the elemental distributions of Pb and Mn and the weaker relationship between Pb and Fe (*Fig. S3*). Zn appeared to be mostly associated with Fe rather than Mn, therefore Zn was not considered further in this manuscript. The relationship between Pb and Mn in the external sediment samples near the cave entrance indicates that sediment Mn phases are also important hosts of Pb outside the cave environment and this warrants further investigation in a future article.

XRD analysis was performed to identify the bulk mineralogy of the Mn oxides. Identification of natural Mn oxide phases is often challenging because of the typical poor crystallinity and presence of silicates and clay minerals as common impurities/co-phases (Potter and Rossman, 1979a) and it is difficult to apply the Rietveld refinement to the XRD data (Julien et al., 2003). The XRD spectrum had broad asymmetric peaks at 7.84 Å, 3.86 Å, 2.42 Å, and 1.41 Å (Fig. 2B). Such spectra are characteristic of hydrated materials with nanoparticulate particle

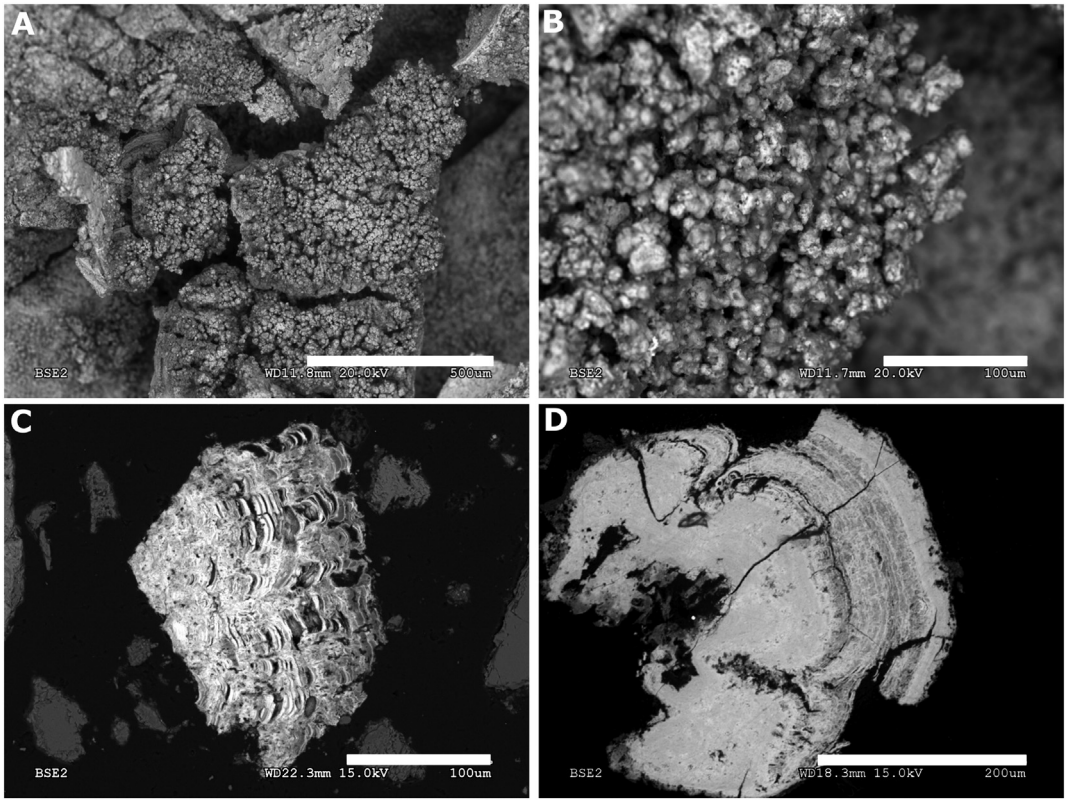

Fig. 1. SEM images of the cave crusts. A (scale bar 500 μm) and B (scale bar 100 μm): BSE images of pebbles sampled from St. Cuthbert's Sump II. C (scale bar 100 μm) and 1D (scale bar 200 μm): BSE images of cave sediment particles (showing polished cross sections of the particles) sampled from Wookey Hole Cave Chambers 2/3. These appear to show concentric layers of growth and are possibly detrital phases, which formed in the upper parts of the cave system (such as Sump II) and washed downstream.

size, poor crystallinity, and with much structural disorder ('turbostatic') (Learman et al., 2011; Potter and Rossman, 1979b, 1979a). The XRD spectrum of the cave mineral is shown to be consistent with the XRD spectrum of synthetic vernadite/birnessite (δ-MnO_2) which was made following the method of Villalobos et al. (2003), including with sorbed Pb (Bacon, 2014) (Fig. 2B).

Raman spectroscopy is useful for characterising poorly crystalline minerals by the presence of diagnostic vibrational bands. Birnessite-type (δ-MnO_2) Mn oxide phases typically feature low Raman activity and have three major features usually at 500–510, 575–585 and 625–650 cm^{-1}, with the two higher bands most dominant (Julien et al., 2003). Raman analyses of the cave crusts further support the identity of the cave deposits as being δ-MnO_2 (*Fig. S4*). The peak for the high band in most of the samples was observed to be slightly higher than that for pure birnessite. A frequency shift of the high-wavenumber stretching mode has, however, been attributed to a function of the interlayer spacing in birnessite-type manganese dioxides (Julien et al., 2003). For the St Cuthbert's Swallet cave samples, this shift is considered to be related to the presence of Pb and Zn forming surface complexes at the vacancy sites (see below). This is supported by a peak shift of the Raman spectrum of synthetic vernadite/birnessite (δ-MnO_2) with sorbed Pb (*Fig. S4*).

The identification of birnessite in St. Cuthbert's Swallet cave system is consistent with studies of other caves around the world, where the predominant natural Mn oxide present is generally birnessite (Potter and

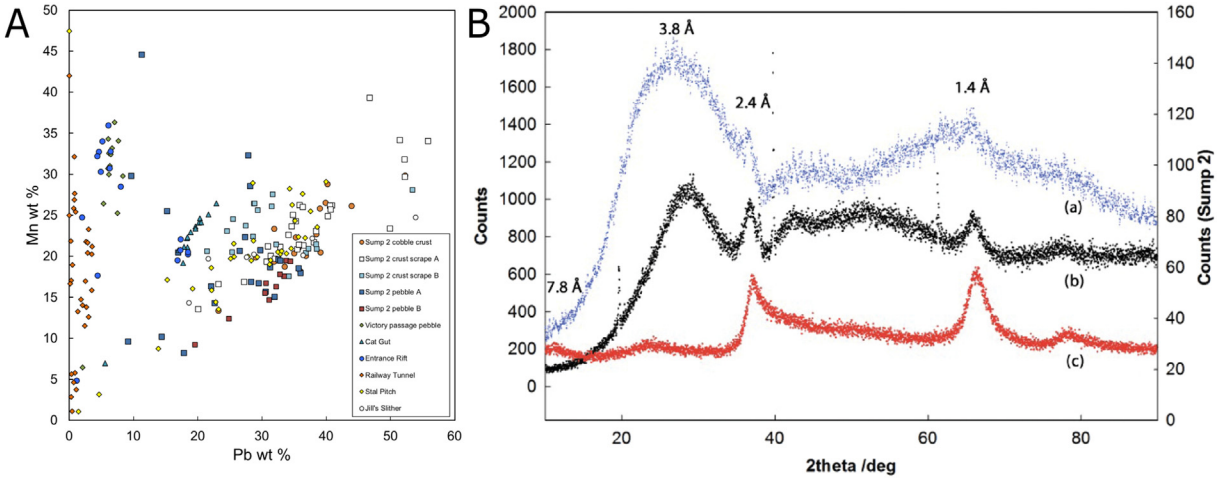

Fig. 2. Characterisation of the Pb-rich Mn cave crusts. A) EDX analysis: element covariance plots of Pb and Mn from cave crust samples, St. Cuthbert's Swallet. B) XRD spectra of: (a) cave crust from St Cuthbert's Swallet Sump II (b) synthetic δ-MnO_2 with high loading of sorbed Pb (46 wt%) and (c) synthetic δ-MnO_2 only.

Rossman, 1979a; Rossi et al., 2010; White et al., 2009). However, it is notable that the high enrichment of heavy metals recorded here exceeds heavy metal enrichments reported previously in other cave systems around the world (e.g. Rossi et al., 2010), making the St Cuthbert's mine and cave system of particular environmental significance.

Birnessite consists of nanoparticulate 2D sheets (phyllomanganates) of edge-sharing Mn(IV) octahedra (MnO_6) The sheets are highly disordered (turbostatic) and have an average thickness of 11 nm and width of 35 nm, separated at 10 Å basal plane spacing by H_2O molecules (Bargar et al., 2009). Surface areas for birnessite are reported to be high: 746 $m^2\ g^{-1}$ (Drits et al., 1997) and 900 $m^2\ g^{-1}$ (Lanson et al., 2000). Aqueous metal species can sorb onto birnessite by forming outer-sphere surface complexes, or inner-sphere surface complexes, above negatively charged structural vacancy sites on the {001} surfaces of the Mn octahedra sheets (Grangeon et al., 2010; Manceau et al., 2002; Villalobos et al., 2005). The particularly high sorption affinity of birnessite for transition metals compared to other sorbent oxides (i.e. goethite) is attributed to birnessite having a low point of zero charge (PZC) of ~2.3, and a high surface area (Matocha et al., 2001; Tonkin et al., 2004). The sorption (surface complexation) reactions between metals and birnessite are dependent on the pH of the solution, have rapid kinetics, and may be the paramount reactions controlling aqueous metal concentrations (and therefore bioaccessibility) in a range of environmental settings (e.g. Beak et al., 2008; Morin et al., 2001; O'Reilly and Hochella, 2003).

In summary, the geochemical and mineralogical analyses revealed that the St Cuthbert's Swallet cave crusts are mainly composed of poorly crystalline birnessite-type (δ-MnO_2) Mn oxide phases that in places hold a substantial mass of Pb and to a lesser extent Zn. The layered texture of the minerals suggests a biogenic origin. EDS analyses showed that Mn and Pb are generally positively correlated, and that the Pb and Zn are distributed throughout the layered crusts, not just on the surface. The varied stoichiometry of the crusts indicates that Pb and Zn are sorbed and incorporated into the birnessite continuously as the oxides form in the stream passages. The proportions of the entrained metals are controlled by the available flux of dissolved metals and solution pH, rather than precipitating as distinct mineral phases such as cerussite ($PbCO_3$) or chalcophonite ($(Zn,Mn,Fe)Mn_2O_5 \cdot n\ H_2O$), which were not observed.

3.2. Microbial community characterisation

3.2.1. Sample description

To characterise the microbial community and the potential for microbial Mn(II)-oxidisers, three samples of brown/black cave crusts and three adjacent samples were collected from the St Cuthbert's Swallet cave system in January 2017. The cave crust samples A2 (Fig. 3A, B) and B4 (Fig. 3D, E) were characterised by SEM and EDS to confirm that they were similar to those previously analysed. Both contained Mn and Pb, with concentrations much higher in Sample A2 (Mn 21 ± 0.4%, Pb 21 ± 1%) compared to Sample B4 (Mn 6 ± 2%, Pb 6 ± 2%). The differences in concentration are likely due to the texture of the crusts; Sample A2 was obtained from a coating on a hard pebble, therefore the subsample analysed was predominantly the Mn crust. Sample B4 was more friable and therefore the subsample contained less crust and more sand and silt. These concentrations were in the same range as previously observed (*Table S2*). Features suggestive of microbes were observed in both samples, including potential fungal hyphae (Fig. 3C) and bacterial cells (Fig. 3F). The samples contained similar amounts of organic carbon, with 0.68% TOC present in Sample A2 and 0.62% in Sample B4.

Table 1
Microbial community abundance and diversity.

	Sample A2	Sample B4	Sample B6
Number of prokaryotic ASVs[a]	1604	3041	2377
Shannon diversity prokaryotes[a]	6.21	7.04	6.66
16S rRNA pg g^{-1} sample	7.71	8.01	3.04
Number of fungal ASVs[b]	260	673	487
Shannon diversity fungi[b]	4.74	5.74	5.65
18S rRNA pg g^{-1} sample	1.36	1.81	0.69

[a] Bacterial sequences were subsampled into 187,032 reads per samples.
[b] Fungal sequences were subsampled into 60,801 reads per samples.

3.2.2. Microbial diversity

DNA was extracted from the three Mn(IV) oxide cave crust samples (A2, B4 and B6), and the marker genes for prokaryotes and fungi were sequenced to characterise the composition and diversity of their microbial communities. Sample A1 was collected adjacent to Sample A2 and was assessed visually to not contain Mn(IV) oxides; DNA extraction was attempted from Sample A1 as a control but the amount recovered was insufficient for sequencing. This may indicate that the prokaryotic and eukaryotic community in the cave materials was insignificant compared to the Mn(IV) oxide crusts.

Prokaryotic diversity in the cave crusts was high, with Shannon indices >6 reported and large numbers of ASVs (Table 1). The quantity of prokaryotic DNA was broadly similar to that for Mn(IV)-oxides in cave systems in the USA, in the order of 5×10^7 copy numbers per gram

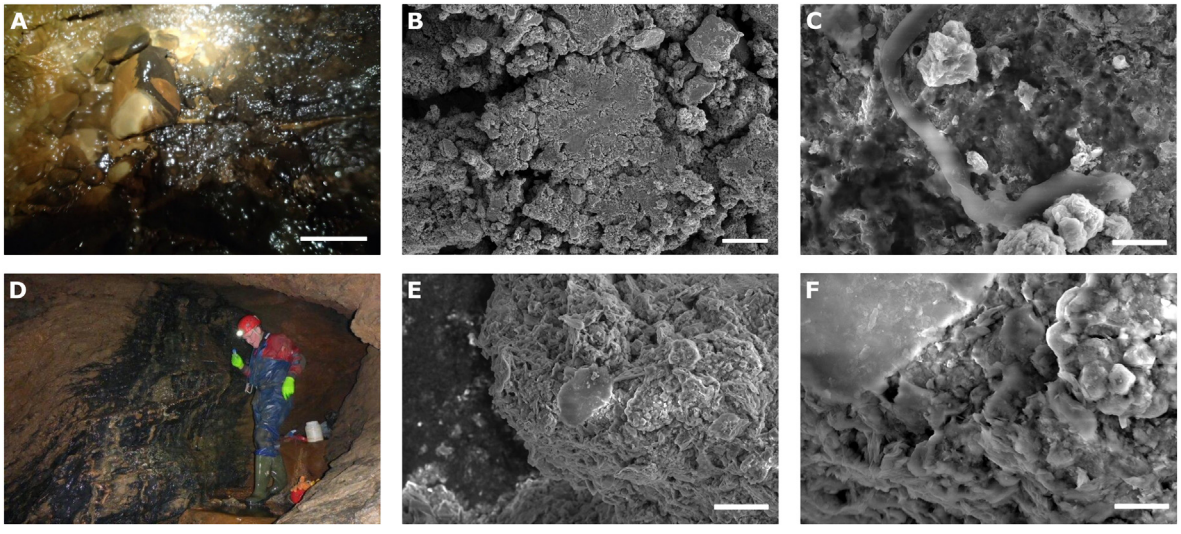

Fig. 3. Cave crust samples. A) Collection of Sample A2, scale bar ~10 cm. B) Sample A2 general texture, SE, scale bar 50 μm. C) Sample A2 possible hyphae, SE, scale bar 5 μm. D) Collection of Sample B4. E) Sample B4 general texture, SE, scale bar 20 μm. F) Sample B4 possible bacterium, SE, scale bar 5 μm.

compared to between 7×10^7 and 2×10^9 copy numbers per gram previously reported (Carmichael, 2012). Together this indicates that the cave crusts contained diverse and abundant prokaryotic communities.

Eukaryotic DNA was also abundant, although around one order of magnitude lower than prokaryotic DNA (Table 1). The abundance of eukaryotic DNA was comparable to that previously reported for fungi in a Mn(IV) oxide cave systems in the USA, with 2×10^6 copy numbers per gram here, compared to between not detected and 6.5×10^7 copy numbers per gram (Carmichael, 2012). The number of fungal ASVs was more variable, with the highest values observed for Sample B4.

There is no indication that the high Pb in Sample A2 (~21%) compared to B4 (~6%) adversely affected the microbial community abundance or diversity, given the amount of DNA was similar in Samples A2 and B4 and there were only slightly fewer prokaryotic ASVs and a slightly lower Shannon index for Sample A2. However Sample A2 did have the fewest fungal ASVs. A previous study observed that the presence of 1–3% Pb in soils impacted on fungal community diversity and richness but not the bacterial community (Hui et al., 2012). The similar increased sensitivity of fungi to metals compared to bacteria may also be reflected in the results from St Cuthbert's Swallet, although more samples would be required to confirm this.

3.2.3. Prokaryotes

At the phylum level, the most abundant bacterial phyla were the Proteobacteria (24–33%), Acidobacteria (17–20%) and Planctomycetes (10–14%) (Fig. 4). The Archaea comprised 3–8% of the prokaryotic community detected, predominantly Thaumarchaeota (3–7%). The results for Samples B4 and B6 appeared broadly similar to each other, perhaps reflecting their collection from the same part of the cave system, Sample A2 was less similar which may be due to its more distant location within the cave. Sample A2 contained 30–40% more Proteobacteria and Planctomycetes than Samples B4 and B6; these are common and diverse phyla frequently found in environmental samples suggesting that transport from the surface environment may be more significant in this area of the cave. On the other hand Sample A2 contained 30–60% fewer Thaumarchaeota, Nitrospirae, Bacteroidetes and Rokubacteria.

The Thaumarchaeota and Nitrospirae phyla formed a substantial proportion of Sample B4 (5.3% and 6.0% respectively) and Sample B6 (7.1% and 4.8%), but were less abundant in Sample A2 (2.7% and 2.1%). The Thaumarchaeota were predominantly Nitrososphaeria, including *Nitrosopumilaceae* (2.7–4.8%), *Nitrososphaeraceae* (0.0–0.9%), and *Nitrosotaleaceae* (0.0–1.9%); all of whose cultivated organisms are aerobic ammonia-oxidising chemolithoautotrophs (Kerou et al., 2016; Könneke et al., 2005; Pester et al., 2012). The Nitrospirae were assigned to *Nitrospira* (2.1–6.0%); a comammox bacterium capable of full nitrification by oxidising both ammonium and nitrite (Daims et al., 2015). This may indicate that inorganic nitrogen-based metabolisms and autotrophy could provide a source of carbon and energy for the cave crust microbial communities. Both phyla have previously been identified in speleothem surfaces from a carbonate cave, with metagenome analyses confirming the presence of ammonia monooxygenase and nitrite oxidoreductase genes (Ortiz et al., 2014). Nitrospirae were also found to make up 5% of the prokaryotic community in waste from a Mn-removing water treatment works (McCann et al., 2015). The cave crust samples did not contain

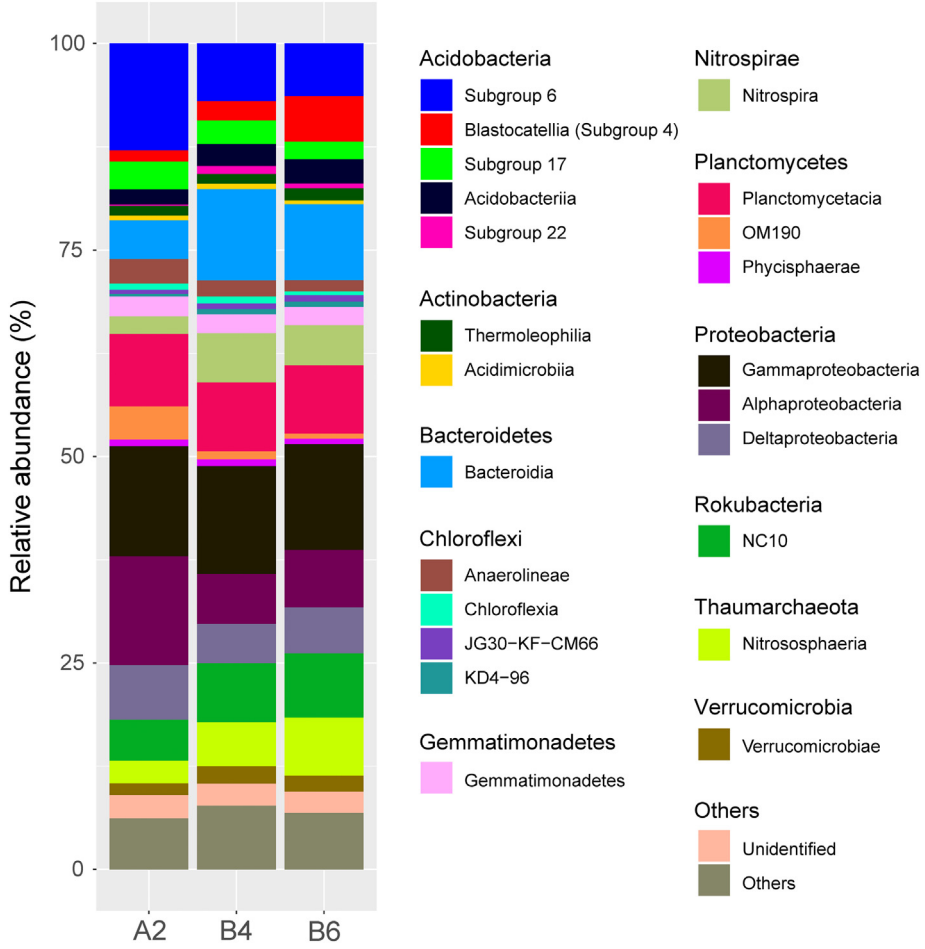

Fig. 4. Phylogenetic diversity for bacteria in the Mn(IV)-oxide cave crusts. Phyla and classes detected >0.5% on average are illustrated. Those <0.5% at the class level are represented as 'others'.

sequences assigned to the *Candidatus* Brocadiales, anaerobic ammonia-oxidising Planctomycetes (van Niftrik and Jetten, 2012), suggesting that aerobic ammonia oxidisers were predominant.

Within the Bacteroidetes phylum, the *Chitinophagaceae* (1.7–5.6%), *Flavobacteriaceae* (0.2–3.3%) and *Microscillaceae* (0.5–1.1%) were the predominant families; these mostly comprise aerobic chemoorganotrophs, although there are some facultative anaerobes (Hahnke et al., 2016; McBride, 2014; Rosenberg, 2014). The Rokubacteria phylum is most closely related to the Nitrospirae (Becraft et al., 2017), and the cave crust sample sequences were assigned to the Rokubacteriales (3.9–5.1%) and *Methylomirabilaceae* (1.0–2.7%). Uncultured Rokubacteriales have previously been identified in karst caves, although at average abundances of <1% (Zhu et al., 2019). The Rokubacteria genome includes genes that encode for aerobic respiration and fermentation, heterotrophy, nitrogen reduction and nitrification, indicating a diverse metabolic potential (Becraft et al., 2017). The *Methylomirabilaceae* are known to contain nitrite-reducing methane-oxidising bacteria (Graf et al., 2018).

At the ASV level, the five most frequently detected ASVs for each sample represented 5.5–9.5% of the prokaryotic community (*Table S3*). Samples B4 and B6 shared two of the most abundant ASVs, whereas Sample A2 did not share any, again perhaps reflecting the different area from which the samples were collected within the cave system. Notably some of the most abundant ASVs were closely related to uncultured prokaryotes from manganese deposits (ASVs 4, 7, 8, 9, 12, 24), cave systems and karst (ASVs 2, 5, 6, 9, 11, 12, 24, 27), and metal-impacted sediments (ASVs 2, 12, 16, 24); conditions which are all relevant to the present study.

In total, the cave crusts contained 86 prokaryotic ASVs assigned to known Mn(II)-oxidising genera, with Mn(II)-oxidisers estimated to make up between 5.2 and 6.3% of the prokaryotic community in the three samples. These included the known heterotrophic Mn(II)-oxidising genera *Terrimonas* (1.2–5.3%), *Flavobacterium* (0.2–3.3%), *Pedomicrobium* (0.3–2.5%), and *Hyphomicrobium* (0.2–0.4%) (Carmichael and Bräuer, 2015). Some of the most abundant ASVs were closely related to bacteria from Mn(IV) minerals, Mn crusts, and Fe—Mn nodules and concretions. Together this indicates that bacteria from Mn(II)-oxidising environments were relatively common, and may have contributed to the formation of the Mn(IV) oxide deposits St Cuthbert's Swallet cave crusts. No evidence was observed for sequences closely related to *Candidatus* Manganitrophus noduliformans - the key chemolithoautotrophic Mn(II)-oxidising bacterium identified by Yu and Leadbetter (2020).

Interestingly, many of the most abundant ASVs were closely related to prokaryotes from a range of soil and water environments from studies on nitrogen cycling, including ammonia oxidation, nitrite oxidation, and ureolysis (ASVs 2, 3, 5, 6, 8, 11, 12, 24, 27) (*Table S3*). For example, ASV3 and ASV5 were closely related to *Candidatus Nitrosopelagicus brevis* strain CN25, an ammonia-oxidising archaeon (Santoro et al., 2015). ASV6 and ASV12 were closely related to uncultured bacteria from studies of ammonia oxidation. ASV24 was assigned to the Betaproteobacteria family *Nitrosomonadaceae*, for which all cultured representatives are lithoautotrophic ammonia oxidisers (Prosser et al., 2014). ASV11 and ASV27 were closely related to *Nitrospira* spp. capable of full nitrification (Daims et al., 2015). In total, at least 7.3–17% of sequences were assigned to ammonia-oxidising prokaryotes (*Nitrosomonadaceae*, Nitrososphaeria, *Nitrospira*), and 2.1–6.0% to the nitrite oxidising *Nitrospira* genus. This suggests that N cycling is likely to play an important role in these cave crusts. A previous study showed that it was possible to add ammonia to stimulate autotrophic nitrifiers to generate small amounts of organic carbon as a waste product, which then acted as a substrate for heterotrophic Mn(II)-oxidisers (Cao et al., 2015). Applying these findings to the St Cuthbert's Swallet cave crusts, suggests that the energy supporting the microbial community growth in the cave crusts could come from autotrophic ammonia oxidation and nitrification.

PICRUSt2 was used to predict the presence of functional genes based on 16S rRNA sequence data. The 10 most abundant functional genes in the samples predicted by PICRUSt2 were mostly housekeeping genes (*Fig. S5A*). To find out more details on potential redox biotransformations, metal resistance and respiratory processes we interrogated the dataset for particular genes that may be involved in these processes (list provided as *Table S4*). Analysis shows that the predicted functional gene abundance profile was very similar for all three samples, suggesting high functional redundancies across the samples (*Fig. S5*). From the selected gene set (*Table S4*), predictions of the most abundant genes reflected the expected functioning of a Mn(IV) oxide microbial community, comprising genes associated with Mn(II)-oxidation, oxidative stress defence (Mn(IV) oxides are highly oxidising) and aerobic respiration (*Fig. S5B*).

Cytochrome *c* oxidase was predicted to be one of the most abundant genes in the samples (0.54–0.58%) (*Fig. S5*). This is a heme group oxidoreductase which has previously been implicated in Mn(II)-oxidation; cytochrome *c* oxidase defective mutants of *Pseudomonas putida* were unable to oxidise Mn(II) but this ability was restored upon complementation of the mutation (Caspi et al., 1998). The gene that encodes for the active Mn oxidase in *Bacillus* spp. (Romano et al., 2017) was not predicted to be present in this dataset.

A number of genes involved in oxidative stress response were also predicted to be present including peroxiredoxin (0.29–0.31%), superoxide dismutase (0.19%), and thioredoxin-disulfide (0.23–0.24%) (*Fig. S5B*). Peroxiredoxins are ubiquitous antioxidant peroxidase enzymes with redox-active cysteine residues that can reduce hydrogen peroxide and may be play a role in protecting against reactive oxygen species (Oláhová et al., 2008). Superoxide dismutase is another antioxidant enzyme that catalyses the transformation of superoxide into O_2 and hydrogen peroxide. Mn(IV) oxides are thought to be formed by oxidation of Mn(II) by microbially-produced superoxide, so it follows that the microbial community is predicted to be able to deal with excess superoxide and hydrogen peroxide that may be present. Both peroxiredoxins and superoxide dismutase have also been linked to heavy metal resistance (Oláhová et al., 2008; Schmidt et al., 2007). Thioredoxin-disulfide reductase is a ubiquitous enzyme involved in the reduction of NADPH to maintain intracellular proteins in a reduced state (Arnér and Holmgren, 2000), and thioredoxins have been shown to control oxidative stress response in bacteria (Zeller and Klug, 2006).

Mn(IV) oxides are commonly formed by heterotrophs, therefore it was unsurprising that the presence of genes associated with aerobic respiration was predicted: for example succinate dehydrogenase (ubiquinone) (0.29–0.30%), pyruvate dehydrogenase (lipoamide) (0.23–0.25%), dihydrolipoyl dehydrogenase (0.19–0.21%), and fumarate hydratase (0.18–0.19%) were all predicted and are part of the glycolysis and tricarboxylic acid cycle. Given that C is often limited in oligotrophic cave environments, and that sequences closely related to known autotrophic ammonia oxidisers were identified, the dataset was also interrogated for the presence of potential marker genes for autotrophic respiration. Genes related to Calvin cycle – phosphoglycerate kinase (0.14–0.15%) and ribulose-bisphosphate carboxylase (0.02–0.03%) – were predicted, demonstrating the potential for autotrophic acquisition of carbon in the cave crust microbial community.

After identifying that putative ammonia and nitrite oxidisers formed a substantial proportion of the prokaryotic community, the dataset was searched for predictions of the genes associated with these processes. Genes associated with ammonia oxidation (Daims et al., 2016), ammonia monooxygenase (0.004–0.011%) and hydroxylamine dehydrogenase (0.0002–0.0012%) were predicted at very low relative abundances in our samples. Gene involved in nitrite oxidation (Caspi, 2012), nitrite reductase (0.019–0.039%), nitric-oxide reductase (0.002–0.007%) and nitrous oxide reductase (0.006–0.011%) were also predicted at very low abundances. Although PICRUSt2 is a powerful tool for predicting functional gene abundances, shotgun metagenomic sequencing could be used to confirm these predictions as part of future studies.

3.2.4. Fungi

The fungal community was identified by ITS sequencing. At the phylum level, the St Cuthbert's Swallet cave crusts were dominated by sequences assigned to the Ascomycota (59–76%), Rozellomycota (4–26%), and Basidiomycota (8–21%), with only 2–4% sequences unassigned based on the UNITE database (Fig. 5). Samples A2, B4 and B6 each appeared to be considerably different at the class level. FUNGuild analysis showed many sequences were assigned to saprotrophs and plant pathogens (*Fig. S6*).

At the ASV level, the five most frequently detected fungal ASVs in each sample represented 11–26% of the community. Samples B4 and B6 shared three of same most abundant ASVs, whereas Sample A2 shared two with Samples B4 and B6 (*Table S5*). Of the most abundant fungal ASVs, two were most closely related to known Mn(II)-oxidising genera (Carmichael and Bräuer, 2015); ASV 519 (1.5–5.5%) was most closely related to *Plectosphaerella* spp. and ASV 42 (0.6–3.7%) to *Cladosporium* spp. (*Table S5*). In addition, three of the most abundant OTUs were assigned to Helotiales (ASV 371, 570, 645), which contain known Mn(II)-oxidisers (Miyata et al., 2006; Schweisfurth, 1971).

In total, 41 ASVs were closely related to known Mn(II)-oxidising genera (Carmichael and Bräuer, 2015; Hofrichter, 2002) representing 9.6–9.9% of the fungal community. These including those assigned to the *Plectosphaerella* (2.9–7.0%), *Cladosporium* (0.6–5.0%), *Acremonium* (0.5–1.3%), *Microdochium* (0.4–0.5%), and *Pyrenochaeta* (0.1–0.6%) genera. This indicates that fungi with the potential for Mn(II)-oxidation were relatively common, and may have contributed to the formation of the Mn(IV) oxide deposits St Cuthbert's Swallet cave crusts. A previous study of Mn oxide-associated microbial communities in mine-water remediation systems (but with no Pb present) showed that the fungal taxonomic profiles correlated better than bacterial communities with Mn removal (Chaput et al., 2015), highlighting the importance of fungi in driving Mn(II)-oxidation these systems.

3.2.5. Summary of microbial community composition

The cave crusts contain abundant and diverse prokaryotic and fungal communities, the composition of which suggests they are capable of respiring using organic and inorganic C and N compounds. A substantial proportion of sequences were closely related to known heterotrophic Mn(II)-oxidising prokaryotes and fungi, and genes that have been implicated in Mn(II)-oxidation formed a substantial proportion of the gene profile predicted by PICRUSt2. Together this highlights the potential for the cave crusts being formed by microbial activity. However, this analysis was performed at the genus level, and although the DNA contained sequences assigned to genera with Mn(II)-oxidisers were present, this does not mean that the Mn(II)-oxidising species were present, nor that they were actively oxidising Mn(II) in the cave crust samples. Therefore, isolation experiments were required to identify if key components of the cave crust microbial community were able to oxidise Mn(II), and if so, could they function in the presence of high concentrations of Pb.

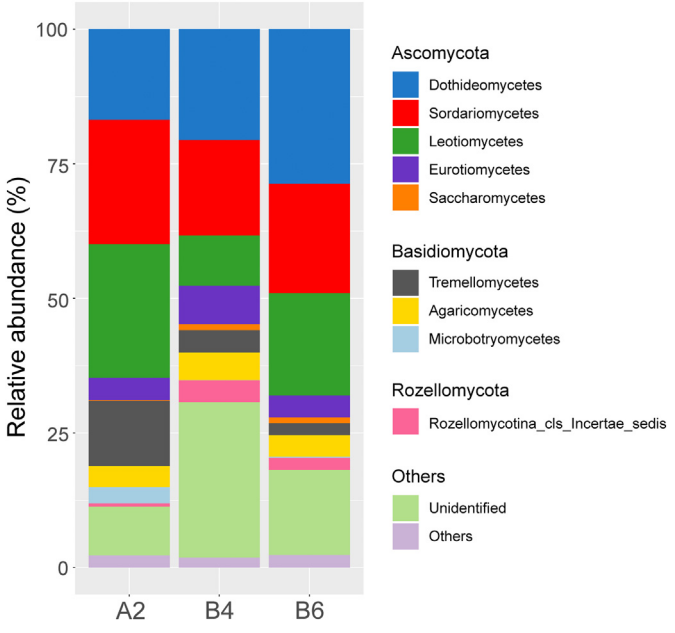

Fig. 5. Phylogenetic diversity for fungi in the Mn(IV)-oxide cave crusts. Phyla and classes detected >0.5% on average are illustrated. Those <0.5% at the class level are represented as 'others'.

The functioning of microbial communities in oligotrophic cave environments clearly warrants further investigation, particularly the role of autotrophic ammonia and nitrite oxidisers. As well as in caves these groups have been identified in various Mn(IV) oxides, including in wastewater remediation systems (Cao et al., 2015; McCann et al., 2015). The interactions between nutrient availability, autotrophic and heterotrophic metabolisms and Mn(II)-oxidation should be explored in future studies, together with the implications for contaminant transport.

3.3. Isolation and enrichment of Mn(II)-oxidising microorganisms

A series of isolation and enrichment experiments were performed to identify the presence of active Mn(II)-oxidising microorganisms in the cave crust samples. Additional experiments were performed to assess whether they could still oxidise Mn(II) in the presence of Pb, to reflect the cave crust environment.

3.3.1. Isolation and identification of Mn(II)-oxidising microorganisms

Freshwater minimal medium agar plates were supplemented with acetate or glucose to stimulate heterotrophic growth in the presence of $Mn(II)Cl_2$. Cultures were observed for colour changes that indicate the formation of typically brown/black Mn(IV) oxides, and the presence of Mn(IV) oxides was confirmed using the LBB dye test.

The acetate and glucose plates were both observed to become colonised by different types of fungi, with visible hyphae. A black coloured fungus was isolated (*Fig. S7*) and Sanger sequencing showed it was closely related to *Cladosporium* sp., a known Mn(II)-oxidiser. However, the isolate did not produce Mn(IV) oxides (LBB dye test), and similar colonies were later observed to form on the control plate. Although sequences closely related to *Cladosporium* spp. were identified in the cave crust samples, it is well known that *Cladosporium* spp. are commonly isolated from air (Bensch et al., 2012). Therefore no further analyses were performed on this fungal isolate.

A fungicide (Nystatin) was subsequently added to the medium to favour the growth of Mn(II)-oxidising prokaryotes. Brown coloured colonies were identified, isolated, and the presence of Mn(IV) oxides confirmed using the LBB dye test (*Fig. S8*). No Mn(IV) oxides formed on the control plates, indicating that abiotic Mn(II)-oxidation was not significant. In total six strains of Mn(II)-oxidising heterotrophic bacteria were isolated, four on glucose plates and two on acetate plates, indicating both organic substrates could support microbial Mn(II)-oxidation (*Table S6*). All of the isolates had a rectangular rod-shaped morphology with cells approximately 1 μm long (Fig. 6).

Three of the isolates (B, D, E) from the glucose plates were most closely related to *Streptomyces ederensis*, suggesting they were the same organism (*Table S6*). Interestingly, they were similarly closely related to a *Streptomyces* sp. isolated on Pb-enriched plates, from a study of siderophore production by metallotolerant bacteria isolated from the rhizosphere (Złoch et al., 2016). SEM imaging showed that Isolates B and D formed straight sporophores (Pridham et al., 1958) (Fig. 6A, C). The presence of extracellular electron-dense minerals was observed using BSE imaging, these varied from a 10 μm well-defined angular crystal structure (Fig. 6B) to a 2 μm rounded cluster (Fig. 6C); both were confirmed to contain Mn using EDS. The other isolate (G) from the

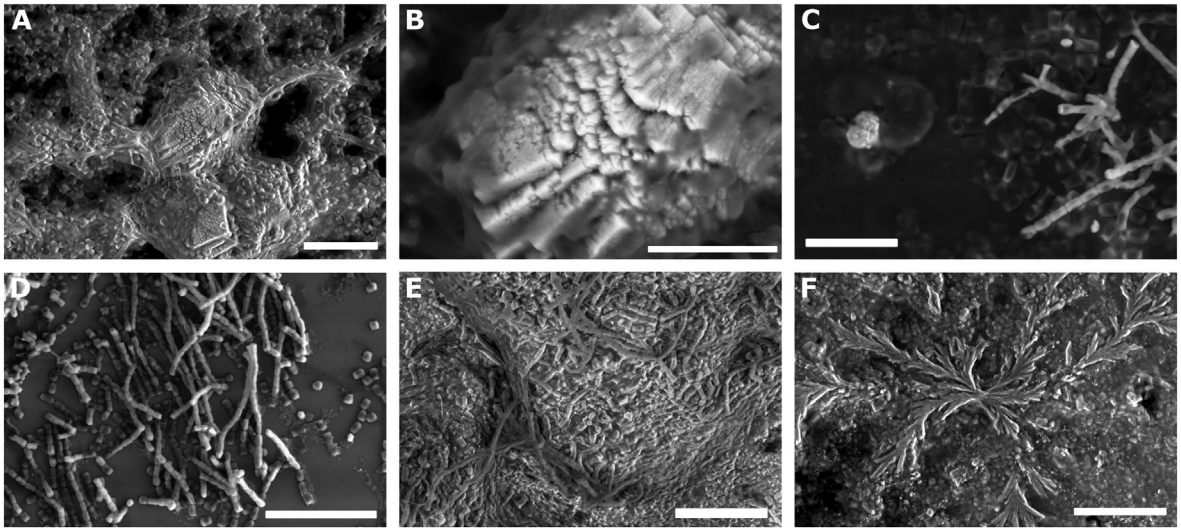

Fig. 6. SEM images of isolates and Mn(IV)-oxides. A) Isolate D (*S. ederensis*), SE, scale bar 10 μm. B) Mineral from the centre of panel A at enhanced magnification, BSE, scale bar 5 μm. C) Isolate B (*S. ederensis*), SE, scale bar 5 μm. D) Isolate G (*P. loti*), SE, scale bar 10 μm. E & 6F) Isolate A (*S. fulvissimus*), SE, scale bars 10 μm.

glucose plates was closely related to *Phyllobacterium loti* (*Table S6*) and formed straight chains (Fig. 6D). Although it was very similar in appearance to Isolate B (Fig. 6C), they were from different phyla (Proteobacteria, Actinobacteria). Both isolates (A, C) from the acetate plates were most closely related to *Streptomyces fulvissimus*, suggesting they were the same organism (*Table S6*). SEM imaging showed Isolate A formed flexuous (Fig. 6E) or biverticillus (Fig. 6F) sporophores (Pridham et al., 1958).

Organisms most closely affiliated with the *Streptomyces* and *Phyllobacterium* genera formed <0.05% of the prokaryotic community sequenced from Sample A2, indicating that a relatively small proportion of the prokaryotic community was represented by the isolates. *Streptomyces* spp. are spore-forming aerobic chemoheterotrophic Actinobacteria, that produce an extensively branched mycelium, can break down complex organic matter and are ubiquitous in soils (Kämpfer, 2006). *Streptomyces* spp. are commonly found in studies of cave environments, and are known superoxide dismutase producers and Mn(II)-oxidisers (Carmichael and Bräuer, 2015; Schmidt et al., 2007; Timonin, 1950). *Phyllobacterium* spp. are part of the Rhizobiales order and are typically aerobic heterotrophs (Willems, 2014), found in association with plants including as endophytes and in the rhizosphere (Mantelin et al., 2006). *Phyllobacterium* spp. have also been isolated from caves (Jurado et al., 2005), but to the best of our knowledge there are no previous data demonstrating that they can produce superoxide dismutase or oxidise Mn(II).

Given the high Pb and Zn content of the cave crusts it is worth noting that both *Streptomyces* and *Phyllobacterium* spp. have both been shown to be metal-resistant. A *Streptomyces* sp. isolate could grow in the presence of 6.3 mM Pb (Zanardini et al., 1997), another isolated from a former U mine site was shown to tolerate a range of heavy metals (Schmidt et al., 2007), and a novel *Streptomyces* sp. (*S. plumbiresistens*) was isolated from lead-contaminated soils and shown to have a minimum inhibitory concentration of 4 mM Pb^{2+} (Guo et al., 2009). *Phyllobacterium* spp. have previously been isolated from the rhizosphere of plants colonising mine tailings and also observed tolerate heavy metals, including 5.8 mM Pb (Ma et al., 2013; Zappelini et al., 2018). Both *Streptomyces* and *Phyllobacterium* spp. secrete siderophores (Ma et al., 2013; Patzer and Braun, 2010), which are known to detoxify heavy metals and benefit microbial communities.

3.3.2. The impact of Pb on the Mn(II)-oxidising isolates

The six isolates were inoculated onto additional freshwater medium plates containing 0.1 mM Pb to investigate the impact of Pb on their growth. All the isolates were observed to grow on freshwater minimal medium plates containing 0.1 mM Pb (*Fig. S9*), suggesting that Pb was not toxic at this concentration. Similar growth was observed on the plates containing 0.1 mM Pb and Mn(II), however, only the four isolates on glucose plates (Isolates B, D, E, G; most closely related to *S. ederensis* and *P. loti*) produced Mn(IV) oxides under these conditions (*Fig. S9*), identified via the LBB dye test. Although the isolates closely related to *S. fulvissimus* could oxidise Mn(II) on acetate plates with no Pb present, they were unable to form Mn(IV) oxides on plates with 0.1 mM Pb. This could be due to variability within the *Streptomyces* genus, or may indicate that glucose respiration had beneficial effects for stimulating microbial Mn(II)-oxidation in the presence of Pb for *Streptomyces* spp.

3.3.3. Enrichment of Mn(II)-oxidising microorganisms

Enrichment experiments were performed by inoculating aliquots of the cave crusts (Sample A2 and B4) into liquid freshwater minimal medium containing Mn(II) and acetate or glucose, as an alternative method to isolate Mn(II)-oxidising microorganisms. Similar results were obtained for the two cave crusts samples, but the outcomes contrasted for the different electron donor amendments.

The acetate-amended experiments showed that Mn(II) was removed from solution, with aqueous concentrations decreasing from an initial 150–190 μM to 0–30 μM after 12 days (Fig. 7A). A slight decrease was also observed in the uninoculated controls, from around 155 to 120 μM, demonstrating a small, but significant amount of abiotic Mn(II)-oxidation occurred. The pH remained circumneutral in the abiotic controls, but increased from 7.0 to 7.8 in the inoculated experiments. This can be explained by the microbial catabolism of acetate to produce bicarbonate, leading to a slight increase in pH. Together these results suggest that acetate amendment stimulated heterotrophic metabolism in the cave crust microbial communities, which enhanced the oxidation of aqueous Mn(II) present in the medium, and its removal from solution as insoluble Mn(IV) oxide minerals.

Conversely, the glucose amended enrichments showed that inoculation with cave crust materials caused Mn(II) to be released to solution, from an initial 100–210 μM to 280–670 μM after 7 days (Fig. 7B). This is likely due to solubilisation of cave crust material by microbial Mn(IV)-reduction coupled to glucose respiration (Lovley et al., 2004). This was somewhat unexpected given the experiments were conducted under oxidising conditions, although rapid switching between Mn(IV)-oxidation and Mn(II)-reduction is known to occur in redox fluctuating conditions, and Mn(IV)-reduction has previously been observed to occur in aerobic incubations (Bratina et al., 1998). Furthermore, previous work

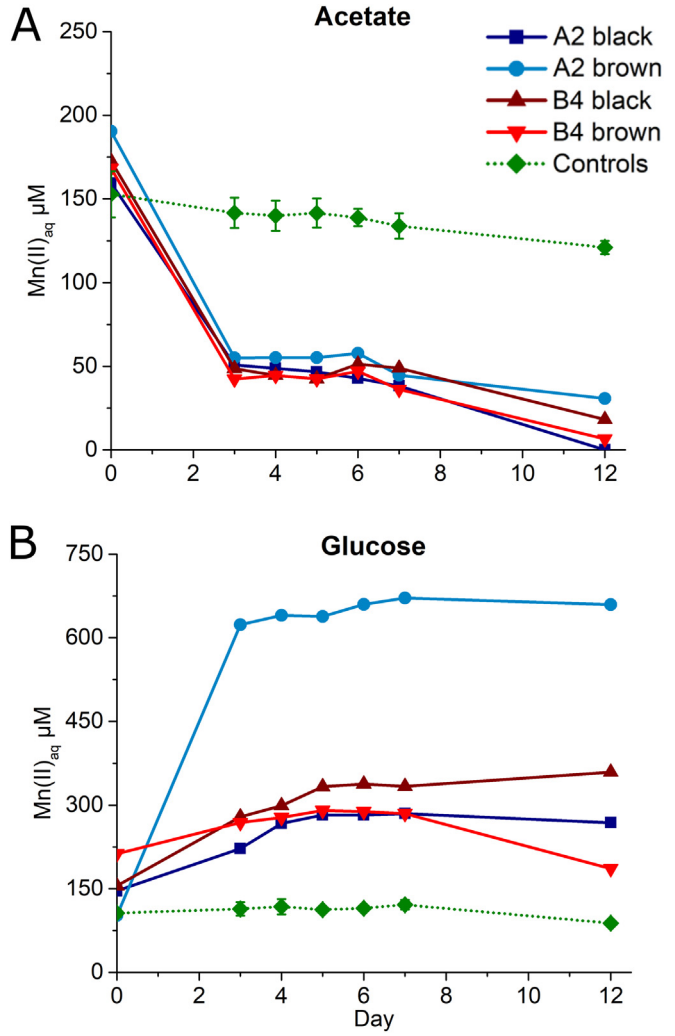

Fig. 7. Cave crust enrichment experiments using two aliquots of Sample A2 and two of Sample B4. A) Acetate amended. B) Glucose amended.

has noted that rich media are not suitable for cultivating Mn(II)-oxidisers due to them being outcompeted by fast-growing heterotrophs (Cao et al., 2015). A considerably larger quantity of aqueous Mn(II) was produced in one of the enrichments from cave crust Sample A2, which may be due to the higher Mn content, heterogeneity in the amount of cave crust added, or the proportion or growth rate of Mn(IV)-reducing microorganisms in the inoculum. Between day 7 and day 12 the concentrations of aqueous Mn(II) decreased slightly in three of the samples (to 190–660 µM), perhaps representing a shift from microbial Mn(IV)-reduction to Mn(II)-oxidation, although concentrations did continued to increase in one of the enrichments from Sample B4.

The controls behaved similarly to the acetate-amended experiments, with a slight decrease observed in the uninoculated controls, from around 110 to 90 µM, again demonstrating a small, but significant amount of abiotic Mn(II)-oxidation occurred. Again the pH remained circumneutral in the abiotic controls, but in the glucose amended inoculated experiments it decreased from 7.0 to 6.5. This can be explained through the aerobic respiration of glucose by microorganisms generating acidity such as through pyruvic acid formation. Together these results demonstrate that amending the cave crust samples with glucose stimulated the release of Mn as aqueous Mn(II), likely via by microbial Mn(IV)-reduction. They support the idea that the availability of substantial quantities of organic matter inhibit microbial Mn(II)-oxidation in an environmental community (Cao et al., 2015), and instead stimulate microbial Mn(IV)-reduction and solubilisation.

3.3.4. Summary of isolation and enrichment of Mn(II)-oxidising microorganisms

Three strains of Mn(II)-oxidising bacteria were isolated from the St Cuthbert's Swallet cave crusts, most closely related to *S. ederensis*, *P. loti* and *S. fulvissimus*. To the best of our knowledge this is the first report of Mn(II)-oxidation by a *Phyllobacterium* spp. All isolates could grow in the presence of Pb, which reflects their known metal-resistance abilities. Although these genera made up a relatively small proportion of the cave crusts, both *S. ederensis*, and *P. loti* were shown to be able to oxidise Mn(II) in the presence of Pb, suggesting that they may play a role in forming the cave Mn oxides deposits.

The enrichment experiments showed that organic carbon availability is likely to control whether Mn(II)-oxidation or Mn(IV)-reduction occurs, with Mn(II)-oxidation favoured under more C-limited conditions. An interesting contrast may be observed by comparing the enrichments and the isolates. In the enrichments glucose amendment led to Mn(IV)-reduction being the dominant processes, observed by the production of aqueous Mn(II). In contrast, glucose agar plates were shown to stimulate Mn(II)-oxidation by the *S. ederensis* and *P. loti* isolates, particularly when Pb was present. This difference could be explained by Mn(II)-oxidation being outcompeted by Mn(IV)-reduction in the enrichments which contained complex microbial communities, while clearly there will be no competition effects when working with isolates.

3.4. Cave waters

Given the substantial amount of Pb incorporated into the cave crusts, and that the capacity for active microbial Mn(II)-oxidation in the presence of Pb has been demonstrated, it is interesting to reflect on how this microbial activity may impact on contaminant transport within the cave system. Historic mining activities contaminated the local surface environment with high levels of Pb (Allison, 2002; British Geological Survey, 2017), which over time have been transported into the cave system and accumulated in the Mn-oxide cave crusts (Fig. 2). To investigate recent cave water geochemistry, six samples were collected and analysed for metals and biogeochemical indicator parameters in January 2017, together with twelve samples analysed for metals (eight samples from 2012 and four from 2013). Concentrations of major anions and cations (*Table S7A*) were similar to values previously reported for the surface streams that supply the cave, except for Ca which was an order of magnitude higher in surface waters (Knights and Stenner, 2001).

For the 2017 samples, the four samples from Location A (*Fig. S1*) and one from Location C were broadly similar, while the sample from Location B was somewhat different (*Table S7A*). Compared to the other water samples, Sample W-B5 had higher concentrations of Na, Cl, K, phosphate, nitrate and sulfate. Higher salt and higher nutrients could either suggest a different source of the water, and/or the closer proximity of Location B to the surface. A previous study of surface water hydrochemistry showed seasonal variations in K and nitrate which were suggested to reflect the use of these nutrients by plants in summer and their release by decaying vegetation in winter (Knights and Stenner, 2001). Interestingly, aqueous nitrite, Mn and Fe were detected in sample W-B5 but not in the other samples, which suggests that the conditions in Location B within the cave might be slightly more reducing. Concentrations of Pb, Zn, As and Cu were also highest in sample W-B5; it is not possible to say whether this was due to the different source of the waters, the location the sample was collected, or the geochemical conditions. Simple short-chain organic acids (acetic and formic acids) were detected in four of the six samples. These are known to provide a source of energy and carbon for heterotrophic growth, and which may favour the growth Mn(II)-oxidising heterotrophs and the formation of Mn(IV) oxides. Unfortunately, we were unable to measure ammonium in our laboratories, to see whether it was present in substantial quantities to support the ammonia-oxidising

community. Previous work, however, found ammonium concentrations in the Mendips region to be <1 mg L^{-1} (Knights and Stenner, 2001).

The St Cuthbert's cave system is spatially complex, and the water flow influenced by historic mining activity and significant hydrological changes in the early 1970s and late 1980s (Stenner, 1997). Nevertheless, metal concentrations were plotted to give an indication of spatial variations throughout the cave system (*Fig. S10*). Although the concentrations of Pb were higher in the 2012/13 dataset compared to 2017 (*Table S7A*, *S7B*), the same general trend was observed. The highest concentrations of Pb were found in the cave waters closest to the entrance and mostly decreased throughout the cave system, until no Pb was detected at the stream resurgence. This trend was also observed in a previous study (Stenner, 1978). One exception to this was the 'Nr Sump 1/Pyrolusite' sample from 2012; this was high in Pb which may have been caused by a higher sampling of colloids (with sorbed Pb) that passed through the filter from a more turbid sample (cavers will inevitably disturb the streambed sediments somewhat in order to move through the passageways).

The dissolved concentrations of Pb and Zn in the cave waters will be controlled by factors such as the relative abundances in the contaminated surface sediments and remaining ore minerals, the relative dissolution or precipitation equilibrium constants and kinetics, as well as the relative sorption affinities with possible sorbent minerals and organic complexes. Assuming that the cave waters are at chemical equilibrium, the measured concentrations of dissolved Pb and Zn were below the saturation concentrations for the dominant Pb and Zn bearing phases in the region: galena (PbS) and sphalerite (ZnFeS). This means that alternative phases or complexes are controlling the dissolved concentrations of Pb and Zn; in this instance it is likely to be the biogenic Mn (IV) oxides (Figs. 2, *S3*).

3.5. A model for the natural attenuation of Pb

Overall the cave water data show that Pb concentrations were highest at the entrance of the cave, and generally decreased throughout the cave system. Sediments and crusts within the cave are highly enriched in Pb (*Table S2* and Stenner, 1979), and concentrations were positively correlated with Mn (Figs. 2, *S3*). This demonstrates that Pb is being removed from solution via sorption onto and accumulation within Mn(IV) oxide deposits. The texture of the Mn oxides was characteristic of biogenic processes (Fig. 1) and tentative fungal hyphae and bacterial cells were observed (Fig. 3). The cave crusts contained highly diverse prokaryotic and fungal communities, including a substantial proportion of DNA sequences closely related to known Mn(II)-oxidising bacteria and fungi (Figs. 4, 5), together with predicted genes for dealing with oxidative stress and metal resistance that would be expected in a Mn(II)-oxidising microbial community. Moreover, Mn(II)-oxidising microorganisms were enriched (Fig. 7A) and isolated (Fig. 6) from the cave crusts, with the isolates shown to actively grow and produce Mn(IV) oxides in the presence of Pb.

Therefore, we propose that microbial Mn(II)-oxidation is actively contributing to the sequestration of Pb in the St Cuthbert's cave system. Pb is removed from groundwater by forming surface complexes onto actively forming microbial Mn(IV) oxide deposits, which act as a filter to naturally attenuate contaminant transport in this system. The microbes benefit from the formation of Mn(IV) oxide minerals as the sorption of Pb extracellularly will offer protection from oxidative stress and other toxic effects caused by contact with heavy metal contamination. The scavenging of trace elements by Mn oxides has been shown to play an important role in reducing the fluxes of a range of contaminants and limit the availability of micronutrients in many other karst caves (M.J. Carmichael et al., 2013; S.K. Carmichael et al., 2013; Dale et al., 2015). Ford and Williams (2007) estimate that approximately 25% of the world's population depends partly, or solely on karst groundwater, therefore the importance of understanding the geochemical controls on the quality of these waters is essential. The formation of Mn(IV) oxides by microbial Mn(II) oxidation also has broader implications in controlling contaminant behaviour in sediments and waters (Hinkle et al., 2017; Kay et al., 2001; Plathe et al., 2013; Sherman and Peacock, 2010), demonstrating the wider environmental relevance of the processes identified in the St Cuthbert's Swallet.

The remobilisation and stability of the Pb in these cave crusts is an important consideration. We tentatively propose that because of the broad experimental sorption edges of Pb on birnessite, (which reach maximum sorption above pH ~5 (Bacon, 2014)), under the ambient circumneutral pH conditions in the caves the Pb surface complexes on the birnessite will remain stable, maintaining the very low dissolved Pb concentrations in the waters. This could be tested in future with experiments whereby cave crust samples are placed in different pH solutions. This can be also assessed with an appropriate and validated surface complexation model (see below). Incidental ingestion of Pb-bearing soils and sediment is a major exposure pathway for Pb. Beak et al. (2008) report that 12 wt% Pb on birnessite was effectively irreversibly bound under conditions of pH 1.8 after 24 h, simulating the human gastrointestinal tract (in vitro). However, desorption of up to 45 wt% Pb from Pb-loaded birnessite was observed to be ~99% fully reversible at pH ~1 after 4 weeks duration (Bacon, 2014). Further research on the possible hysteresis and kinetics of Pb sorption/desorption on birnessite under a range of loadings and conditions is therefore needed. The Pb-loaded cave crusts can also be dislodged over time by the stream water, and there is evidence that over time this material has been transported downstream and deposited within the sediment of the River Axe valley (Bacon, 2014). Reductive dissolution of the birnessite under more reducing redox conditions may also liberate Pb. Further experimental work on the stability of the Pb-bearing birnessite cave samples under different environmental conditions is needed to assess this possible remobilisation mechanism.

To assess whether surface complexation of Pb (and Zn) onto birnessite in the soils and sediment of the Mendip caves is controlling the observed dissolved concentrations, and to test whether these surface complexes are stable under the current (and alternative) geochemical conditions simple K_d models will not suffice; surface complexation models are needed (Bethke and Brady, 2000). These require a molecular-level understanding of the surface complexation structures (i.e. coordination) and surface site properties, as well as the mass action expressions and corresponding equilibrium constants (Sherman, 2009; Wang and Giammar, 2013). Surface complexation models have rarely been applied for simulating sorption as part of contaminant fate and transport studies, owing to a dearth of structural information for the specific interaction(s), as well as insufficient evidence to support including such models. Appropriate surface complexation models of Pb/Zn onto birnessite are essential for further investigation of the natural attenuation given by these cave deposits, and such work is in preparation for future publication.

4. Conclusions

The St Cuthbert's Swallet cave is an interesting and possibly unique cave ecosystem where the natural attenuation of environmental Pb-contamination is occurring. The Mn(IV) oxide cave crusts were highly enriched in Pb, yet contained diverse and abundant microbial communities, with many sequences closely related to known Mn(II)-oxidising prokaryotes and fungi. Isolation experiments confirmed that active Mn(II)-oxidation by bacteria from the *Streptomyces* and *Phyllobacterium* genera was possible, including in the presence of Pb.

Microbial Mn(II)-oxidation requires a source of energy and carbon, which are not always readily available in oligotrophic cave systems. In St Cuthbert's Swallet, there is evidence for trace amounts of organic acids (up to 1.8 μM acetate and 1.5 μM formate) in some groundwaters that could support heterotrophic growth. Indeed our enrichment experiments showed that acetate stimulated the formation of Mn(IV) oxides, but excess organics caused Mn(IV)-reduction to dominate and the

mobilisation of Mn(II). As well as this, the role of C fixation by autotrophic ammonia and nitrite oxidation is likely to be important in the St Cuthbert's cave crusts, and the waste products from this process provide a source of energy and C to support the Mn(II)-oxidising microbial community. Given that these ammonia and nitrite oxidisers have been identified in other Mn(IV) oxide deposits, further exploration of links these groups is clearly warranted, as is the impact of the availability of organic substrates on controlling these natural attenuation processes. It would also be interesting to undertake further isolation experiments using the methods of Yu and Leadbetter (2020) to observe whether the cave crusts contain chemolithoautotrophic Mn(II)-oxidising bacteria.

In summary, the biogeochemical conditions in St Cuthbert's Swallet favour microbial Mn(II)-oxidation and the active sequestration of Pb from groundwaters, representing a natural analogue from where lessons can be learned to aid the design of remediation systems for metal-impacted waters.

CRediT authorship contribution statement

Laura Newsome: Conceptualization, Methodology, Formal analysis, Investigation, Writing – original draft, Visualisation, Funding acquisition. **Charles Bacon**: Formal analysis and Investigation (mineralogy), Writing – original draft. **Hokyung Song**: Formal analysis (PICRUSt2), Writing – review & editing, Visualisation. **Yunyao Luo**: Investigation (isolation and enrichments). **David Sherman**: Writing – review & editing (mineralogy), Funding acquisition. **Jonathan Lloyd**: Methodology (isolation and enrichments), Writing – review & editing, Funding acquisition.

Funding

This work was supported by an Early Career Research Bursary from the Environmental Mineralogy Group of the Mineralogical Society of Great Britain and Ireland, and by the Natural Environment Research Council (NE/M011518/1, GELYSN1505, GELYSN1525). NERC-CASE partners Golder Associates (UK) Ltd. provided additional sponsorship to CGDB. We used beam line X05LA (Microfocus XAS) at the Swiss Light Source (SLS) and the experiment number was 20120336.

Declaration of competing interest

The authors declare that they have no known competing financial interests or personal relationships that could have appeared to influence the work reported in this paper.

Acknowledgements

We are very grateful to Stuart McManus and the Bristol Exploration Club for collecting the samples from St Cuthbert's Swallet. We would additionally like to thank Paul Lythgoe, Alastair Bewsher (University of Manchester) for analytical support with ICP-AES, ICP-MS, ion chromatography and TOC, and Christopher Boothman (University of Manchester) for assistance with Sanger sequencing. Thanks also to Dr Sally Griffin (nee Allison), the staff of Wookey Hole Caves for access to the caves for sediment sampling, and Dr Chung Choi (University of Bristol) for assistance with analytical procedures.

Published in memory of the late Dr Roger Stenner who pioneered the geochemical exploration of the Mendip Caves, and directly inspired this work.

Appendix A. Supplementary data

Supplementary materials comprising additional methodological information, 7 tables and 10 figures can be found online at https://doi.org/10.1016/j.scitotenv.2020.142312. Nucleotide sequence data are available in the GenBank database under the BioProject accession number PRJNA638888, and the other data are available via Mendeley Data (http://dx.doi.org/10.17632/9cfmwj7ghp.1).

References

Allison, S., 2002. Distribution and Biogeochemical Cycling of Trace Metals in Soils at an Abandoned Lead Mining and Smelting Complex (Priddy, Somerset, England). (PhD Thesis). Bath Spa University.

Anderson, C.R., Johnson, H.A., Caputo, N., Davis, R.E., Torpey, J.W., Tebo, B.M., 2009. Mn(II) oxidation is catalyzed by heme peroxidases in "*Aurantimonas manganoxydans*" strain SI85-9A1 and *Erythrobacter* sp. strain SD-21. Appl. Environ. Microbiol. 75, 4130–4138. https://doi.org/10.1128/AEM.02890-08.

Arnér, E.S.J., Holmgren, A., 2000. Physiological functions of thioredoxin and thioredoxin reductase. Eur. J. Biochem. 267, 6102–6109. https://doi.org/10.1046/j.1432-1327.2000.01701.x.

Bacon, C.G.D., 2014. Surface Complexation of Pb and Zn Onto Birnessite (δ-MnO_2): Soils and Groundwater Controls on Pollution in Soils and Groundwater. (PhD Thesis). University of Bristol.

Bargar, J.R., Fuller, C.C., Marcus, M.A., Brearley, A.J., Perez De la Rosa, M., Webb, S.M., Caldwell, W.A., 2009. Structural characterization of terrestrial microbial Mn oxides from Pinal Creek. AZ. Geochim. Cosmochim. Acta 73, 889–910. https://doi.org/10.1016/j.gca.2008.10.036.

Beak, D.G., Basta, N.T., Scheckel, K.G., Traina, S.J., 2008. Linking solid phase speciation of Pb sequestered to birnessite to oral Pb bioaccessibility: implications for soil remediation. Environ. Sci. Technol. 42, 779–785. https://doi.org/10.1021/es071733n.

Becraft, E.D., Woyke, T., Jarett, J., Ivanova, N., Godoy-Vitorino, F., Poulton, N., Brown, J.M., Brown, J., Lau, M.C.Y., Onstott, T., Eisen, J.A., Moser, D., Stepanauskas, R., 2017. Rokubacteria: genomic giants among the uncultured bacterial phyla. Front. Microbiol. 8, 2264. https://doi.org/10.3389/fmicb.2017.02264.

Bensch, K., Braun, U., Groenewald, J.Z., Crous, P.W., 2012. The genus *Cladosporium*. Stud. Mycol. 72, 1–401. https://doi.org/10.3114/sim0003.

Bethke, C.M., Brady, P.V., 2000. How the Kd approach undermines ground water cleanup. Ground Water 38, 435–443. https://doi.org/10.1111/j.1745-6584.2000.tb00230.x.

Bolyen, E., Rideout, J.R., Dillon, M.R., Bokulich, N.A., Abnet, C.C., Al-Ghalith, G.A., Alexander, H., Alm, E.J., Arumugam, M., Asnicar, F., Bai, Y., Bisanz, J.E., Bittinger, K., Brejnrod, A., Brislawn, C.J., Brown, C.T., Callahan, B.J., Caraballo-Rodríguez, A.M., Chase, J., Cope, E.K., Da Silva, R., Diener, C., Dorrestein, P.C., Douglas, G.M., Durall, D.M., Duvallet, C., Edwardson, C.F., Ernst, M., Estaki, M., Fouquier, J., Gauglitz, J.M., Gibbons, S.M., Gibson, D.L., Gonzalez, A., Gorlick, K., Guo, J., Hillmann, B., Holmes, S., Holste, H., Huttenhower, C., Huttley, G.A., Janssen, S., Jarmusch, A.K., Jiang, L., Kaehler, B.D., Kang, K. Bin, Keefe, C.R., Keim, P., Kelley, S.T., Knights, D., Koester, I., Kosciolek, T., Kreps, J., Langille, M.G.I., Lee, J., Ley, R., Liu, Y.X., Loftfield, E., Lozupone, C., Maher, M., Marotz, C., Martin, B.D., McDonald, D., McIver, L.J., Melnik, A.V., Metcalf, J.L., Morgan, S.C., Morton, J.T., Naimey, A.T., Navas-Molina, J.A., Nothias, L.F., Orchanian, S.B., Pearson, T., Peoples, S.L., Petras, D., Preuss, M.L., Pruesse, E., Rasmussen, L.B., Rivers, A., Robeson, M.S., Rosenthal, P., Segata, N., Shaffer, M., Shiffer, A., Sinha, R., Song, S.J., Spear, J.R., Swafford, A.D., Thompson, L.R., Torres, P.J., Trinh, P., Tripathi, A., Turnbaugh, P.J., Ul-Hasan, S., van der Hooft, J.J.J., Vargas, F., Vázquez-Baeza, Y., Vogtmann, E., von Hippel, M., Walters, W., Wan, Y., Wang, M., Warren, J., Weber, K.C., Williamson, C.H.D., Willis, A.D., Xu, Z.Z., Zaneveld, J.R., Zhang, Y., Zhu, Q., Knight, R., Caporaso, J.G., 2019. Reproducible, interactive, scalable and extensible microbiome data science using QIIME 2. Nat. Biotechnol. https://doi.org/10.1038/s41587-019-0209-9.

Boujelben, N., Bouzid, J., Elouear, Z., 2009. Removal of lead(II) ions from aqueous solutions using manganese oxide-coated adsorbents: characterization and kinetic study. Adsorpt. Sci. Technol. 27, 177–191. https://doi.org/10.1260/026361709789625252.

Bratina, B.J.O., Stevenson, B.S., Green, W.J., Schmidt, T.M., 1998. Manganese reduction by microbes from oxic regions of the Lake Vanda (Antarctica) water column. Appl. Environ. Microbiol. 64, 3791–3797. https://doi.org/10.1128/aem.64.10.3791-3797.1998.

British Geological Survey, 2017. Priddy|locality areas|foundations of the Mendips. [WWW Document]. URL. https://www.bgs.ac.uk/mendips/localities/priddy.html. (Accessed 20 April 2020).

Brown, A.E., Muthumeenakshi, S., Sreenivasaprasad, S., Mills, P.R., Swinburne, T.R., 1993. A PCR primer-specific to *Cylindrocarpon heteronema* for detection of the pathogen in apple wood. FEMS Microbiol. Lett. 108, 117–120.

Bussche, J. Vanden, Soares, E.V., 2011. Lead induces oxidative stress and phenotypic markers of apoptosis in *Saccharomyces cerevisiae*. Appl. Microbiol. Biotechnol. 90, 679–687. https://doi.org/10.1007/s00253-010-3056-7.

Callahan, B.J., Mcmurdie, P.J., Rosen, M.J., Han, A.W., Johnson, A.J., Holmes, S.P., 2016. DADA2 paper supplementary information: high resolution sample inference from amplicon data. Nat. Methods, 0–14 https://doi.org/10.1101/024034.

Cao, L.T.T., Kodera, H., Abe, K., Imachi, H., Aoi, Y., Kindaichi, T., Ozaki, N., Ohashi, A., 2015. Biological oxidation of Mn(II) coupled with nitrification for removal and recovery of minor metals by downflow hanging sponge reactor. Water Res. 68, 545–553. https://doi.org/10.1016/j.watres.2014.10.002.

Caporaso, J.G., Lauber, C.L., Walters, W.A., Berg-Lyons, D., Lozupone, C.A., Turnbaugh, P.J., Fierer, N., Knight, R., 2011. Global patterns of 16S rRNA diversity at a depth of millions of sequences per sample. Proc. Natl. Acad. Sci. U. S. A. 108, 4516–4522. https://doi.org/10.1073/pnas.1000080107.

Caporaso, J.G., Lauber, C.L., Walters, W.A., Berg-Lyons, D., Huntley, J., Fierer, N., Owens, S.M., Betley, J., Fraser, L., Bauer, M., Gormley, N., Gilbert, J.A., Smith, G., Knight, R., 2012. Ultra-high-throughput microbial community analysis on the Illumina HiSeq and MiSeq platforms. ISME J. 6, 1621–1624. https://doi.org/10.1038/ismej.2012.8.

Carmichael, M.J., 2012. Geomicrobiology of Ferromanganese Deposits in Caves of the Upper Tennessee River Basin. (MSc thesis). Appalachian State University.

Carmichael, S.K., Bräuer, S.L., 2015. Microbial diversity and manganese cycling: a review of manganese-oxidizing microbial cave communities. In: Engel, A.S. (Ed.), Microbial Life of Cave Systems. Walter de Gruyter Gmbh, Berlin/Boston, p. 352.
Carmichael, M.J., Carmichael, S.K., Santelli, C.M., Strom, A., Bräuer, S.L., 2013a. Mn(II)-oxidizing bacteria are abundant and environmentally relevant members of ferromanganese deposits in caves of the upper Tennessee river basin. Geomicrobiol J. 30, 779–800. https://doi.org/10.1080/01490451.2013.769651.
Carmichael, S.K., Carmichael, M.J., Strom, A., Johnson, K.W., Roble, L.A., Gao, Y., Bräuer, S.L., 2013b. Sustained anthropogenic impact in Carter Saltpeter Cave, Carter County, Tennessee and the potential effects on manganese cycling. J. Cave Karst Stud. 75, 189–204. https://doi.org/10.4311/2012MB0267.
Carpenter, R.H., Hayes, W.B., 1980. Annual accretion of Fe-Mn-oxides and certain associated metals in a stream environment. Chem. Geol. 29, 249–259. https://doi.org/10.1016/0009-2541(80)90023-6.
Carpenter, R.H., Robinson, G.D., Hayes, W.B., 1978. Partitioning of manganese, iron, copper, zinc, lead, cobalt, and nickel in black coatings on stream boulders in the vicinity of the Magruder mine, Lincoln Co., Georgia. J. Geochem. Explor. 10, 75–89. https://doi.org/10.1016/0375-6742(78)90006-7.
Caspi, R., 2012. MetaCyc nitrifier denitrification. [WWW Document]. URL. https://biocyc.org/META/NEW-IMAGE?type=PATHWAY&object=PWY-7084. (Accessed 18 May 2020).
Caspi, R., Tebo, B.M., Haygood, M.G., 1998. c-Type cytochromes and manganese oxidation in Pseudomonas putida MnB1. Appl. Environ. Microbiol. 64, 3549–3555. https://doi.org/10.1128/aem.64.10.3549-3555.1998.
Chaput, D.L., Hansel, C.M., Burgos, W.D., Santelli, C.M., 2015. Profiling microbial communities in manganese remediation systems treating coal mine drainage. Appl. Environ. Microbiol. 81, 2189–2198. https://doi.org/10.1128/AEM.03643-14.
Daims, H., Lebedeva, E.V., Pjevac, P., Han, P., Herbold, C., Albertsen, M., Jehmlich, N., Palatinszky, M., Vierheilig, J., Bulaev, A., Kirkegaard, R.H., Von Bergen, M., Rattei, T., Bendinger, B., Nielsen, P.H., Wagner, M., 2015. Complete nitrification by *Nitrospira* bacteria. Nature 528, 504–509. https://doi.org/10.1038/nature16461.
Daims, H., Lücker, S., Wagner, M., 2016. A new perspective on microbes formerly known as nitrite-oxidizing bacteria. Trends Microbiol. 24, 699–712. https://doi.org/10.1016/j.tim.2016.05.004.
Dale, J., Harrison, T., Roe, P., Ryder, P., 2015. Britain's longest maze cave: Hudgill Burn Mine Caverns, Cumbria, UK. Cave Karst Sci. 42, 20–41.
Daly, M.J., Gaidamakova, E.K., Matrosova, V.Y., Vasilenko, A., Zhai, M., Venkateswaran, A., Hess, M., Omelchenko, M.V., Kostandarithes, H.M., Makarova, K.S., Wackett, L.P., Fredrickson, J.K., Ghosal, D., 2004. Accumulation of Mn(II) in *Deinicoccus radiodurans* facilitates gamma-radiation resistance. Science (80-.) 306, 1025–1028. https://doi.org/10.1126/science.1103185.
Dong, D., Derry, L.A., Lion, L.W., 2003. Pb scavenging from a freshwater lake by Mn oxides in heterogeneous surface coating materials. Water Res. 37, 1662–1666. https://doi.org/10.1016/S0043-1354(02)00556-0.
Douglas, G., 2019. PICRUSt2 Tutorial (v2.2.0 beta) · picrust/picrust2 Wiki · GitHub. [WWW Document]. URL. https://github.com/picrust/picrust2/wiki/PICRUSt2-Tutorial-(v2.2.0-beta). (Accessed 1 May 2020).
Douglas, G., 2020. Key limitations · picrust/picrust2 Wiki · GitHub. [WWW Document]. URL. https://github.com/picrust/picrust2/wiki/Key-Limitations. (Accessed 12 May 2020).
Douglas, G.M., Maffei, V.J., Zaneveld, J., Yurgel, S.N., Brown, J.R., Taylor, C.M., Huttenhower, C., Langille, M.G.I., 2019. PICRUSt2: an improved and extensible approach for metagenome inference. bioRxiv, 672295 https://doi.org/10.1101/672295.
Drits, V.A., Silvester, E., Gorshkov, A.I., Manceau, A., 1997. Structure of synthetic monoclinic Na-rich birnessite and hexagonal birnessite: I. Results from X-ray diffraction and selected-area electron diffraction. Am. Mineral. 82, 946–961. https://doi.org/10.2138/am-1997-9-1012.
Duckworth, O.W., Sposito, G., 2005. Siderophore-manganese (III) interactions. I. Air-oxidation of manganese(II) promoted by desferrioxamine B. Environ. Sci. Technol. 39, 6037–6044. https://doi.org/10.1021/es050275k.
Ford, D., Williams, P., 2007. Karst Hydrogeology and Geomorphology, Karst Hydrogeology and Geomorphology. John Wiley and Sons Ltd, Dordrecht, Netherlands https://doi.org/10.1002/9781118684986.
Gardes, M., Bruns, T.D., 1993. ITS primers with enhanced specificity for basidiomycetes—application to the identification of mycorrhizae and rusts. Mol. Ecol. 2, 113–118.
Gázquez, F., Calaforra, J.M., Forti, P., 2011. Black Mn-Fe crusts as markers of abrupt palaeoenvironmental changes in El Soplao Cave (Cantabria, Spain). Int. J. Speleol. 40, 163–169. https://doi.org/10.5038/1827-806X.40.2.8.
Gázquez, F., Calaforra, J.M., Rull, F., 2012. Boxwork and ferromanganese coatings in hypogenic caves: an example from Sima de la Higuera Cave (Murcia, SE Spain). Geomorphology 177–178, 158–166. https://doi.org/10.1016/j.geomorph.2012.07.022.
Geszvain, K., Butterfield, C., Davis, R.E., Madison, A.S., Lee, S.-W., Parker, D.L., Soldatova, A., Spiro, T.G., Luther, G.W., Tebo, B.M., 2012. The molecular biogeochemistry of manganese(II) oxidation. Biochem. Soc. Trans. 40, 1244–1248. https://doi.org/10.1042/BST20120229.
Graf, J.S., Mayr, M.J., Marchant, H.K., Tienken, D., Hach, P.F., Brand, A., Schubert, C.J., Kuypers, M.M.M., Milucka, J., 2018. Bloom of a denitrifying methanotroph, '*Candidatus Methylomirabilis limnetica*', in a deep stratified lake. Environ. Microbiol. 20, 2598–2614. https://doi.org/10.1111/1462-2920.14285.
Grangeon, S., Lanson, B., Miyata, N., Tani, Y., Manceau, A., 2010. Structure of nanocrystalline phyllomanganates produced by freshwater fungi. Am. Mineral. 95, 1608–1616. https://doi.org/10.2138/am.2010.3516.
Guo, J.K., Lin, Y.B., Zhao, M.L., Sun, R., Wang, T.T., Tang, M., Wei, G.H., 2009. *Streptomyces plumbiresistens* sp. nov., a lead-resistant actinomycete isolated from lead-polluted soil in north-west China. Int. J. Syst. Evol. Microbiol. 59, 1326–1330. https://doi.org/10.1099/ijs.0.004713-0.
Hahnke, R.L., Meier-Kolthoff, J.P., García-López, M., Mukherjee, S., Huntemann, M., Ivanova, N.N., Woyke, T., Kyrpides, N.C., Klenk, H.P., Göker, M., 2016. Genome-based taxonomic classification of Bacteroidetes. Front. Microbiol. 7. https://doi.org/10.3389/fmicb.2016.02003.
Hansel, C.M., Zeiner, C.A., Santelli, C.M., Webb, S.M., 2012. Mn(II) oxidation by an ascomycete fungus is linked to superoxide production during asexual reproduction. Proc. Natl. Acad. Sci. U. S. A. 109, 12621–12625. https://doi.org/10.1073/pnas.1203885109.
Hinkle, M.A.G., Dye, K.G., Catalano, J.G., 2017. Impact of Mn(II)-manganese oxide reactions on Ni and Zn speciation. Environ. Sci. Technol. 51, 3187–3196. https://doi.org/10.1021/acs.est.6b04347.
Hofrichter, M., 2002. Review: lignin conversion by manganese peroxidase (MnP). Enzym. Microb. Technol. https://doi.org/10.1016/S0141-0229(01)00528-2.
Hui, N., Liu, X.-X., Kurola, J., Mikola, J., Romantschuk, M., 2012. Lead (Pb) contamination alters richness and diversity of the fungal, but not the bacterial community in pine forest soil. Boreal Environ. Res. 17, 46–58.
Irwin, D.J., 1991. St. Cuthbert's Swallet. Bristol Exploration Club.
Julien, C., Massot, M., Baddour-Hadjean, R., Franger, S., Bach, S., Pereira-Ramos, J.P., 2003. Raman spectra of birnessite manganese dioxides. Solid State Ionics 159, 345–356. https://doi.org/10.1016/S0167-2738(03)00035-3.
Jurado, V., Laiz, L., Gonzalez, J.M., Hernandez-Marine, M., Valens, M., Saiz-Jimenez, C., 2005. *Phyllobacterium catacumbae* sp. nov., a member of the order "Rhizobiales" isolated from Roman catacombs. Int. J. Syst. Evol. Microbiol. 55, 1487–1490. https://doi.org/10.1099/ijs.0.63402-0.
Kämpfer, P., 2006. The family *Streptomycetaceae*. In: Dworkin, M., Falkow, S., Rosenberg, E., Schleifer, K., Stackebrandt, E. (Eds.), The Prokaryotes. Springer New York, New York, NY, pp. 538–604 https://doi.org/10.1007/0-387-30743-5_22.
Kay, J.T., Conklin, M.H., Fuller, C.C., O'Day, P.A., 2001. Processes of nickel and cobalt uptake by a manganese oxide forming sediment in Pinal Creek, Globe mining district, Arizona. Environ. Sci. Technol. 35, 4719–4725. https://doi.org/10.1021/es010514d.
Kerou, M., Eloy Alves, R.J., Schleper, C., 2016. Nitrososphaeria. Bergey's Manual of Systematics of Archaea and Bacteria. John Wiley & Sons, Ltd, Chichester, UK, pp. 1–8 https://doi.org/10.1002/9781118960608.cbm00055.
Knights, A.V., Stenner, R.D., 2001. Hydrochemistry of streams which enter St. Cuthbert's Swallet, Priddy, Somerset. Proc. Univ. Bristol Spelæological Soc. 22, 157–181.
Könneke, M., Bernhard, A.E., De La Torre, J.R., Walker, C.B., Waterbury, J.B., Stahl, D.A., 2005. Isolation of an autotrophic ammonia-oxidizing marine archaeon. Nature 437, 543–546. https://doi.org/10.1038/nature03911.
Kozich, J.J., Westcott, S.L., Baxter, N.T., Highlander, S.K., Schloss, P.D., 2013. Development of a dual-index sequencing strategy and curation pipeline for analyzing amplicon sequence data on the MiSeq Illumina sequencing platform. Appl. Environ. Microbiol. 79, 5112–5120. https://doi.org/10.1128/AEM.01043-13.
Kushwaha, A., Hans, N., Kumar, S., Rani, R., 2018. A critical review on speciation, mobilization and toxicity of lead in soil-microbe-plant system and bioremediation strategies. Ecotoxicol. Environ. Saf. https://doi.org/10.1016/j.ecoenv.2017.09.049.
Lane, D.J., 1991. 16S/23S rRNA sequencing. In: Stackebrant, E., Goodfellow, M. (Eds.), Nucleic Acid Techniques in Bacterial Systematics. John Wiley & Sons Ltd, London, pp. 115–175.
Lanson, B., Drits, V.A., Silvester, E., Manceau, A., 2000. Structure of H-exchanged hexagonal birnessite and its mechanism of formation from Na-rich monoclinic buserite at low pH. Am. Mineral. 85, 826–838. https://doi.org/10.2138/am-2000-5-625.
Learman, D.R., Wankel, S.D., Webb, S.M., Martinez, N., Madden, A.S., Hansel, C.M., 2011. Coupled biotic-abiotic Mn(II) oxidation pathway mediates the formation and structural evolution of biogenic Mn oxides. Geochim. Cosmochim. Acta 75, 6048–6063. https://doi.org/10.1016/j.gca.2011.07.026.
Liang, X., Kierans, M., Ceci, A., Hillier, S., Gadd, G.M., 2016. Phosphatase-mediated bioprecipitation of lead by soil fungi. Environ. Microbiol. 18, 219–231. https://doi.org/10.1111/1462-2920.13003.
Lovley, D.R., Phillips, E.J.P., Gorby, Y.A., Landa, E.R., 1991. Microbial reduction of uranium. Nature 350, 413–416.
Lovley, D.R., Holmes, D.E., Nevin, K.P., 2004. Dissimilatory Fe(III) and Mn(IV) reduction. In: Poole, R.K. (Ed.), Advances in Microbial Physiology. Academic Press, pp. 219–286 https://doi.org/10.1016/s0065-2911(04)49005-5.
Ma, Y., Rajkumar, M., Luo, Y., Freitas, H., 2013. Phytoextraction of heavy metal polluted soils using *Sedum plumbizincicola* inoculated with metal mobilizing *Phyllobacterium myrsinacearum* RC6b. Chemosphere 93, 1386–1392. https://doi.org/10.1016/j.chemosphere.2013.06.077.
Manceau, A., Lanson, B., Drits, V.A., 2002. Structure of heavy metal sorbed birnessite. Part III: results from powder and polarized extended X-ray absorption fine structure spectroscopy. Geochim. Cosmochim. Acta 66, 2639–2663. https://doi.org/10.1016/S0016-7037(02)00869-4.
Mantelin, S., Fischer-Le Saux, M., Zakhia, F., Béna, G., Bonneau, S., Jeder, H., de Lajudie, P., Cleyet-Marel, J.C., 2006. Emended description of the genus *Phyllobacterium* and description of four novel species associated with plant roots: *Phyllobacterium bourgognense* sp. nov., *Phyllobacterium ifriqiyense* sp. nov., *Phyllobacterium leguminum* sp. nov. Int. J. Syst. Evol. Microbiol. 56, 827–839. https://doi.org/10.1099/ijs.0.63911-0.
Matocha, C.J., Elzinga, E.J., Sparks, D.L., 2001. Reactivity of Pb(II) at the Mn(III,IV) (oxyhydr)oxide-water interface. Environ. Sci. Technol. 35, 2967–2972. https://doi.org/10.1021/es0012164.
McBride, M.J., 2014. The family *Flavobacteriaceae*. The Prokaryotes: Other Major Lineages of Bacteria and the Archaea. Springer-Verlag, Berlin Heidelberg, pp. 643–676 https://doi.org/10.1007/978-3-642-38954-2_130.
McCann, C.M., Gray, N.D., Tourney, J., Davenport, R.J., Wade, M., Finlay, N., Hudson-Edwards, K.A., Johnson, K.L., 2015. Remediation of a historically Pb contaminated soil using a model natural Mn oxide waste. Chemosphere 138, 211–217. https://doi.org/10.1016/j.chemosphere.2015.05.054.

McKenzie, R.M., 1980. The adsorption of lead and other heavy metals on oxides of manganese and iron. Aust. J. Soil Res. 18, 61–73. https://doi.org/10.1071/SR9800061.
Medlin, L., Elwood, H.J., Stickel, S., Sogin, M.L., 1988. The characterization of enzymatically amplified eukaryotic 16S-like rRNA-coding regions. Gene 71, 491–499. https://doi.org/10.1016/0378-1119(88)90066-2.
Miyata, N., Maruo, K., Tani, Y., Tsuno, H., Seyama, H., Soma, M., Iwahori, K., 2006. Production of biogenic manganese oxides by anamorphic Ascomycete fungi isolated from streambed pebbles. Geomicrobiol J. 23, 63–73. https://doi.org/10.1080/01490450500533809.
Morin, G., Juillot, F., Ildefonse, P., Calas, G., Samama, J.C., Chevallier, P., Brown, G.E., 2001. Mineralogy of lead in a soil developed on a Pb-mineralized sandstone (Largentière, France). Am. Mineral. 86, 92–104. https://doi.org/10.2138/am-2001-0110.
NCBI, 2015. NCBI insights: accessing the hidden kingdom: fungal ITS reference dequences NCBI insights. [WWW Document]. URL. https://ncbiinsights.ncbi.nlm.nih.gov/2015/05/11/accessing-the-hidden-kingdom-fungal-its-reference-sequences-2/. (Accessed 24 May 2020).
NCBI, 2020. BLAST: basic local alignment search tool. [WWW Document]. URL. https://blast.ncbi.nlm.nih.gov/Blast.cgi. (Accessed 1 May 2020).
Nealson, K.H., 2006. The manganese-oxidizing bacteria. In: Dworkin, M., Falkow, S., Rosenberg, E., Schleifer, K., Stackebrandt, E. (Eds.), The Prokaryotes. Springer New York, New York, NY, pp. 222–231 https://doi.org/10.1007/0-387-30745-1_11.
Nguyen, N.H., Song, Z., Bates, S.T., Branco, S., Tedersoo, L., Menke, J., Schilling, J.S., Kennedy, P.G., 2016. FUNGuild: an open annotation tool for parsing fungal community datasets by ecological guild. Fungal Ecol. 20, 241–248. https://doi.org/10.1016/j.funeco.2015.06.006.
van Niftrik, L., Jetten, M.S.M., 2012. Anaerobic ammonium-oxidizing bacteria: unique microorganisms with exceptional properties. Microbiol. Mol. Biol. Rev. 76, 585–596. https://doi.org/10.1128/mmbr.05025-11.
Nilsson, R.H., Larsson, K.-H., Taylor, A.F.S., Bengtsson-Palme, J., Jeppesen, T.S., Schigel, D., Kennedy, P., Picard, K., Glöckner, F.O., Tedersoo, L., Saar, I., Kõljalg, U., Abarenkov, K., 2019. The UNITE database for molecular identification of fungi: handling dark taxa and parallel taxonomic classifications. Nucleic Acids Res. 47, D259–D264. https://doi.org/10.1093/nar/gky1022.
Northup, D.E., Lavoie, K.H., 2001. Geomicrobiology of caves: a review. Geomicrobiol J. 18, 199–222. https://doi.org/10.1080/01490450152467750.
O'Connor, D., Hou, D., Ok, Y.S., Lanphear, B.P., 2020. The effects of iniquitous lead exposure on health. Nat. Sustain. https://doi.org/10.1038/s41893-020-0475-z.
Oláhová, M., Taylor, S.R., Khazaipoul, S., Wang, J., Morgan, B.A., Matsumoto, K., Blackwell, T.K., Veal, E.A., 2008. A redox-sensitive peroxiredoxin that is important for longevity has tissue- and stress-specific roles in stress resistance. Proc. Natl. Acad. Sci. U. S. A. 105, 19839–19844. https://doi.org/10.1073/pnas.0805507105.
O'Reilly, S.E., Hochella, M.F., 2003. Lead sorption efficiencies of natural and synthetic Mn and Fe-oxides. Geochim. Cosmochim. Acta 67, 4471–4487. https://doi.org/10.1016/S0016-7037(03)00413-7.
Ortiz, M., Legatzki, A., Neilson, J.W., Fryslie, B., Nelson, W.M., Wing, R.A., Soderlund, C.A., Pryor, B.M., Maier, R.M., 2014. Making a living while starving in the dark: metagenomic insights into the energy dynamics of a carbonate cave. ISME J. 8, 478–491. https://doi.org/10.1038/ismej.2013.159.
Patzer, S.I., Braun, V., 2010. Gene cluster involved in the biosynthesis of griseobactin, a catechol-peptide siderophore of *Streptomyces* sp. ATCC 700974. J. Bacteriol. 192, 426–435. https://doi.org/10.1128/JB.01250-09.
Pester, M., Rattei, T., Flechl, S., Gröngröft, A., Richter, A., Overmann, J., Reinhold-Hurek, B., Loy, A., Wagner, M., 2012. *amoA*-based consensus phylogeny of ammonia-oxidizing archaea and deep sequencing of *amoA* genes from soils of four different geographic regions. Environ. Microbiol. 14, 525–539. https://doi.org/10.1111/j.1462-2920.2011.02666.x.
Plathe, K.L., Lee, S.W., Tebo, B.M., Bargar, J.R., Bernier-Latmani, R., 2013. Impact of microbial Mn oxidation on the remobilization of bioreduced U(IV). Environ. Sci. Technol. 47, 3606–3613.
Potter, R.M., Rossman, G.R., 1979a. Mineralogy of manganese dendrites and coatings. Am. Mineral. 64, 1219–1226.
Potter, R.M., Rossman, G.R., 1979b. The tetravalent manganese oxides: identification, hydration, and structural relationships by infrared spectroscopy. Am. Mineral. 64, 1199–1218.
Pridham, T.G., Hesseltine, C.W., Benedict, R.G., 1958. A guide for the classification of *Streptomycetes* according to selected groups. Appl. Microbiol. 189, 109–114.
Prosser, J.I., Head, I.M., Stein, L.Y., 2014. The family *Nitrosomonadaceae*. The Prokaryotes: Alphaproteobacteria and Betaproteobacteria. Springer-Verlag, Berlin Heidelberg, pp. 901–918 https://doi.org/10.1007/978-3-642-30197-1_372.
QIIME2docs, 2020. "Moving pictures" tutorial — QIIME 2 2020.2.0 documentation. [WWW Document]. URL. https://docs.qiime2.org/2020.2/tutorials/moving-pictures/. (Accessed 1 May 2020).
Quast, C., Pruesse, E., Yilmaz, P., Gerken, J., Schweer, T., Yarza, P., Peplies, J., Glöckner, F.O., 2013. The SILVA ribosomal RNA gene database project: improved data processing and web-based tools. Nucleic Acids Res. 41, D590–D596. https://doi.org/10.1093/nar/gks1219.
Rensing, C., Sun, Y., Mitra, B., Rosen, B.P., 1998. Pb(II)-translocating P-type ATPases. J. Biol. Chem. 273, 32614–32617. https://doi.org/10.1074/jbc.273.49.32614.
Roane, T.M., Pepper, I.L., Gentry, T.J., 2015. Microorganisms and metal pollutants. Environmental Microbiology, Third edition Elsevier Inc, pp. 415–439 https://doi.org/10.1016/B978-0-12-394626-3.00018-1.
Romano, C.A., Zhou, M., Song, Y., Wysocki, V.H., Dohnalkova, A.C., Kovarik, L., Paša-Tolić, L., Tebo, B.M., 2017. Biogenic manganese oxide nanoparticle formation by a multimeric multicopper oxidase Mnx. Nat. Commun. 8, 1–8. https://doi.org/10.1038/s41467-017-00896-8.
Rosenberg, E., 2014. The family *Chitinophagaceae*. The Prokaryotes: Other Major Lineages of Bacteria and the Archaea. Springer-Verlag, Berlin Heidelberg, pp. 493–495 https://doi.org/10.1007/978-3-642-38954-2_137.
Rossi, C., Lozano, R.P., Isanta, N., Hellstrom, J., 2010. Manganese stromatolites in caves: El Soplao (Cantabria, Spain). Geology 38, 1119–1122. https://doi.org/10.1130/G31283.1.
Santoro, A.E., Dupont, C.L., Richter, R.A., Craig, M.T., Carini, P., McIlvin, M.R., Yang, Y., Orsi, W.D., Moran, D.M., Saito, M.A., 2015. Genomic and proteomic characterization of "*Candidatus Nitrosopelagicus brevis*": an ammonia-oxidizing archaeon from the open ocean. Proc. Natl. Acad. Sci. U. S. A. 112, 1173–1178. https://doi.org/10.1073/pnas.1416223112.
Schalk, I.J., Hannauer, M., Braud, A., 2011. New roles for bacterial siderophores in metal transport and tolerance. Environ. Microbiol. https://doi.org/10.1111/j.1462-2920.2011.02556.x.
Schmidt, Astrid, Schmidt, André, Haferburg, G., Kothe, E., 2007. Superoxide dismutases of heavy metal resistant *Streptomycetes*. J. Basic Microbiol. 47, 56–62. https://doi.org/10.1002/jobm.200610213.
Schweisfurth, R., 1971. Manganoxidierende Pilze I. Vorkommen, Isolierungen und mikroskopische Untersuchungen. Z. Allg. Mikrobiol. 11, 415–430. https://doi.org/10.1002/jobm.19710110506.
Sharma, J., Shamim, K., Dubey, S.K., Meena, R.M., 2017. Metallothionein assisted periplasmic lead sequestration as lead sulfite by <i>Providencia vermicola<i> strain SJ2A. Sci. Total Environ. 579, 359–365. https://doi.org/10.1016/j.scitotenv.2016.11.089.
Sherman, D.M., 2009. Surface complexation modeling: Mineral fluid equilbria at the molecular scale. In: Oelkers, E.H., Schott, J. (Eds.), Reviews in Mineralogy and Geochemistry, Thermodynamics and Kinetics of Water-Rock Interaction. Mineralogical Society of America, pp. 181–205 https://doi.org/10.2138/rmg.2009.70.5.
Sherman, D.M., Peacock, C.L., 2010. Surface complexation of Cu on birnessite (δ-MnO_2): controls on Cu in the deep ocean. Geochim. Cosmochim. Acta 74, 6721–6730. https://doi.org/10.1016/j.gca.2010.08.042.
Stanaway, J.D., Afshin, A., Gakidou, E., Lim, S.S., Abate, D., Abate, K.H., Abbafati, C., Abbasi, N., Abbastabar, H., Abd-Allah, F., Abdela, J., Abdelalim, A., Abdollahpour, I., Abdulkader, R.S., Abebe, M., Abebe, Z., Abera, S.F., Abil, O.Z., Abraha, H.N., Abrham, A.R., Abu-Raddad, L.J., Abu-Rmeileh, N.M.E., Accrombessi, M.M.K., Acharya, D., Acharya, P., Adamu, A.A., Adane, A.A., Adebayo, O.M., Adedoyin, R.A., Adekanmbi, V., Ademi, Z., Adetokunboh, O.O., Adib, M.G., Admasie, A., Adsuar, J.C., Afanvi, K.A., Afarideh, M., Agarwal, G., Aggarwal, A., Aghayan, S.A., Agrawal, A., Agrawal, S., Ahmadi, A., Ahmadi, M., Ahmadieh, H., Ahmed, M.B., Aichour, A.N., Aichour, I., Aichour, M.T.E., Akbari, M.E., Akinyemiju, T., Akseer, N., Al-Aly, Z., Al-Eyadhy, A., Al-Mekhlafi, H.M., Alahdab, F., Alam, K., Alam, S., Alam, T., Alashi, A., Alavian, S.M., Alene, K.A., Ali, K., Ali, S.M., Alijanzadeh, M., Alizadeh-Navaei, R., Aljunid, S.M., Alkerwi, A., Alla, F., Alsharif, U., Altirkawi, K., Alvis-Guzman, N., Amare, A.T., Ammar, W., Anber, N.H., Anderson, J.A., Andrei, C.L., Androudi, S., Animut, M.D., Anjomshoa, M., Ansha, M.G., Antó, J.M., Antonio, C.A.T., Anwari, P., Appiah, L.T., Appiah, S.C.Y., Arabloo, J., Aremu, O., Ärnlöv, J., Artaman, A., Aryal, K.K., Asayesh, H., Ataro, Z., Ausloos, M., Avokpaho, E.F.G.A., Awasthi, A., Quintanilla, B.P.A., Ayer, R., Ayuk, T.B., Azzopardi, P.S., Babazadeh, A., Badali, H., Badawi, A., Balakrishnan, K., Bali, A.G., Ball, K., Ballew, S.H., Banach, M., Banoub, J.A.M., Barac, A., Barker-Collo, S.L., Bärnighausen, T.W., Barrero, L.H., Basu, S., Baune, B.T., Bazargan-Hejazi, S., Bedi, N., Beghi, E., Behzadifar, Masoud, Behzadifar, Meysam, Béjot, Y., Bekele, B.B., Bekru, E.T., Belay, E., Belay, Y.A., Bell, M.L., Bello, A.K., Bennett, D.A., Bensenor, I.M., Bergeron, G., Berhane, A., Bernabe, E., Bernstein, R.S., Beuran, M., Beyranvand, T., Bhala, N., Bhalla, A., Bhattarai, S., Bhutta, Z.A., Biadgo, B., Bijani, A., Bikbov, B., Bilano, V., Bililign, N., Sayeed, M.S. Bin, Bisanzio, D., Biswas, T., Bjorge, T., Blacker, B.F., Bleyer, A., Borschmann, R., Bou-Orm, I.R., Boufous, S., Bourne, R., Brady, O.J., Brauer, M., Brazinova, A., Breitborde, N.J.K., Brenner, H., Briko, A.N., Britton, G., Brugha, T., Buchbinder, R., Burnett, R.T., Busse, R., Butt, Z.A., Cahill, L.E., Cahuana-Hurtado, L., Campos-Nonato, I.R., Cárdenas, R., Carreras, G., Carrero, J.J., Carvalho, F., Castaneda-Orjuela, C.A., Rivas, J.C., Castro, F., Catalá-López, F., Causey, K., Cercy, K.M., Cerin, E., Chaiah, Y., Chang, H.Y., Chang, J.C., Chang, K.L., Charlson, F.J., Chattopadhyay, A., Chattu, V.K., Chee, M.L., Cheng, C.Y., Chew, A., Chiang, P.P.C., Chimed-Ochir, O., Chin, K.L., Chitheer, A., Choi, J.Y.J., Chowdhury, R., Christensen, H., Christopher, D.J., Chung, S.C., Cicuttini, F.M., Cirillo, M., Cohen, A.J., Collado-Mateo, D., Cooper, C., Cooper, O.R., Coresh, J., Cornaby, L., Cortesi, P.A., Cortinovis, M., Costa, M., Cousin, E., Criqui, M.H., Cromwell, E.A., Cundiff, D.K., Daba, A.K., Dachew, B.A., Dadi, A.F., Damasceno, A.A.M., Dandona, L., Dandona, R., Darby, S.C., Dargan, P.I., Daryani, A., Gupta, Rajat Das, Neves, J. Das, Dasa, T.T., Dash, A.P., Davitoiu, D.V., Davletov, K., De La Cruz-Góngora, V., La Hoz, F.P. De, Leo, D. De, Neve, J.W. De, Degenhardt, L., Deiparine, S., Dellavalle, R.P., Demoz, G.T., Denova-Gutiérrez, E., Deribe, K., Dervenis, N., Deshpande, A., Jarlais, D.C.D., Dessie, G.A., Deveber, G.A., Dey, S., Dharmaratne, S.D., Dhimal, M., Dinberu, M.T., Ding, E.L., Diro, H.D., Djalalinia, S., Do, H.P., Dokova, K., Doku, D.T., Doyle, K.E., Driscoll, T.R., Dubey, M., Dubljanin, E., Duken, E.E., Duncan, B.B., Duraes, A.R., Ebert, N., Ebrahimi, H., Ebrahimpour, S., Edvardsson, D., Effiong, A., Eggen, A.E., Bcheraoui, C. El, El-Khatib, Z., Elyazar, I.R., Enayati, A., Endries, A.Y., Er, B., Erskine, H.E., Eskandarieh, S., Esteghamati, A., Estep, K., Fakhim, H., Faramarzi, M., Fareed, M., Farid, T.A., Farinha, C.S.E., Farioli, A., Faro, A., Farvid, M.S., Farzaei, M.H., Fatima, B., Fay, K.A., Fazaeli, A.A., Feigin, V.L., Feigl, A.B., Fereshtehnejad, S.M., Fernandes, E., Fernandes, J.C., Ferrara, G., Ferrari, A.J., Ferreira, M.L., Filip, I., Finger, J.D., Fischer, F., Foigt, N.A., Foreman, K.J., Fukumoto, T., Fullman, N., Fürst, T., Furtado, J.M., Futran, N.D., Gall, S., Gallus, S., Gamkrelidze, A., Ganji, M., Garcia-Basteiro, A.L., Gardner, W.M., Gebre, A.K., Gebremedhin, A.T., Gebremichael, T.G., Gelano, T.F., Geleijnse, J.M., Geramo, Y.C.D., Gething, P.W., Gezae, K.E., Ghadimi, R., Ghadiri, K., Falavarjani, K.G., Ghasemi-Kasman, M., Ghimire, M., Ghosh, R., Ghoshal, A.G., Giampaoli, S., Gill, P.S., Gill, T.K., Gillum, R.F., Ginawi, I.A., Giussani, G., Gnedovskaya, E.V., Godwin, W.W., Goli, S., Gómez-Dantés, H., Gona, P.N., Gopalani, S.V., Goulart, A.C., Grada, A., Grams, M.E., Grosso, G., Gugnani, H.C., Guo, Y., Gupta, Rahul, Gupta,

Rajeev, Gupta, T., Gutiérrez, R.A., Gutiérrez-Torres, D.S., Haagsma, J.A., Habtewold, T.D., Hachinski, V., Hafezi-Nejad, N., Hagos, T.B., Hailegiyorgis, T.T., Hailu, G.B., Haj-Mirzaian, Arvin, Haj-Mirzaian, Arya, Hamadeh, R.R., Hamidi, S., Handal, A.J., Hankey, G.J., Hao, Y., Harb, H.L., Harikrishnan, S., Haro, J.M., Hassankhani, H., Hassen, H.Y., Havmoeller, R., Hawley, C.N., Hay, S.I., Hedayatizadeh-Omran, A., Heibati, B., Heidari, B., Heidari, M., Hendrie, D., Henok, A., Heredia-Pi, I., Herteliu, C., Heydarpour, F., Heydarpour, S., Hibstu, D.T., Higazi, T.B., Hilawe, E.H., Hoek, H.W., Hoffman, H.J., Hole, M.K., Rad, E.H., Hoogar, P., Hosgood, H.D., Hosseini, S.M., Hosseinzadeh, M., Hostiuc, M., Hostiuc, S., Hoy, D.G., Hsairi, M., Hsiao, T., Hu, G., Hu, H., Huang, J.J., Hussen, M.A., Huynh, C.K., Iburg, K.M., Ikeda, N., Ilesanmi, O.S., Iqbal, U., Irvani, S.S.N., Irvine, C.M.S., Islam, S.M.S., Islami, F., Jackson, M.D., Jacobsen, K.H., Jahangiry, L., Jahanmehr, N., Jain, S.K., Jakovljevic, M., James, S.L., Jassal, S.K., Jayatilleke, A.U., Jeemon, P., Jha, R.P., Jha, V., Ji, J.S., Jonas, J.B., Jonnagaddala, J., Shushtari, Z.J., Joshi, A., Jozwiak, J.J., Jürisson, M., Kabir, Z., Kahsay, A., Kalani, R., Kanchan, T., Kant, S., Kar, C., Karami, M., Matin, B.K., Karch, A., Karema, C., Karimi, N., Karimi, S.M., Kasaeian, A., Kassa, D.H., Kassa, G.M., Kassa, T.D., Kassebaum, N.J., Katikireddi, S.V., Kaul, A., Kawakami, N., Kazemi, Z., Karyani, A.K., Kefale, A.T., Keiyoro, P.N., Kemp, G.R., Kengne, A.P., Keren, A., Kesavachandran, C.N., Khader, Y.S., Khafaei, B., Khafaie, M.A., Khajavi, A., Khalid, N., Khalil, I.A., Khan, G., Khan, M.S., Khan, M.A., Khang, Y.H., Khater, M.M., Khazaei, M., Khazaie, H., Khoja, A.T., Khosravi, A., Khosravi, M.H., Kiadaliri, A.A., Kiirithio, D.N., Kim, C. Il, Kim, D., Kim, Y.E., Kim, Y.J., Kimokoti, R.W., Kinfu, Y., Kisa, A., Kissimova-Skarbek, K., Kivimäki, M., Knibbs, L.D., Knudsen, A.K.S., Kochhar, S., Kokubo, Y., Kolola, T., Kopec, J.A., Kosen, S., Koul, P.A., Koyanagi, A., Kravchenko, M.A., Krishan, K., Krohn, K.J., Kromhout, H., Defo, B.K., Bicer, B.K., Kumar, G.A., Kumar, M., Kuzin, I., Kyu, H.H., Lachat, C., Lad, D.P., Lad, S.D., Lafranconi, A., Lalloo, R., Lallukka, T., Lami, F.H., Lang, J.J., Lansingh, V.C., Larson, S.L., Latifi, A., Lazarus, J.V., Lee, P.H., Leigh, J., Leili, M., Leshargie, C.T., Leung, J., Levi, M., Lewycka, S., Li, S., Li, Y., Liang, J., Liang, X., Liao, Y., Liben, M.L., Lim, L.L., Linn, S., Liu, S., Lodha, R., Logroscino, G., Lopez, A.D., Lorkowski, S., Lotufo, P.A., Lozano, R., Lucas, T.C.D., Lunevicius, R., Ma, S., Macarayan, E.R.K., Machado, Í.E., Madotto, F., Mai, H.T., Majdan, M., Majdzadeh, R., Majeed, A., Malekzadeh, R., Malta, D.C., Mamun, A.A., Manda, A.L., Manguerra, H., Mansournia, M.A., Mantovani, L.G., Maravilla, J.C., Marcenes, W., Marks, A., Martin, R.V., Martins, S.C.O., Martins-Melo, F.R., März, W., Marzan, M.B., Massenburg, B.B., Mathur, M.R., Mathur, P., Matsushita, K., Maulik, P.K., Mazidi, M., Mcalinden, C., Mcgrath, J.J., Mckee, M., Mehrotra, R., Mehta, K.M., Mehta, V., Meier, T., Mekonnen, F.A., Melaku, Y.A., Melese, A., Melku, M., Memiah, P.T.N., Memish, Z.A., Mendoza, W., Mengistu, D.T., Mensah, G.A., Mensink, G.B.M., Mereta, S.T., Meretoja, A., Meretoja, T.J., Mestrovic, T., Mezgebe, H.B., Miazgowski, B., Miazgowski, T., Millear, A.I., Miller, T.R., Miller-Petrie, M.K., Mini, G.K., Mirarefin, M., Mirica, A., Mirrakhimov, E.M., Misganaw, A.T., Mitiku, H., Moazen, B., Mohajer, B., Mohammad, K.A., Mohammadi, M., Mohammadifard, N., Mohammadnia-Afrouzi, M., Mohammed, S., Mohebi, F., Mokdad, A.H., Molokhia, M., Momeniha, F., Monasta, L., Moodley, Y., Moradi, G., Moradi-Lakeh, M., Moradinazar, M., Moraga, P., Morawska, L., Morgado-Da-costa, J., Morrison, S.D., Moschos, M.M., Mouodi, S., Mousavi, S.M., Mozaffarian, D., Mruts, K.B., Muche, A.A., Muchie, K.F., Mueller, U.O., Muhammed, O.S., Mukhopadhyay, S., Muller, K., Musa, K.I., Mustafa, G., Nabhan, A.F., Naghavi, M., Naheed, A., Nahvijou, A., Naik, G., Naik, N., Najafi, F., Nangia, V., Nansseu, J.R., Nascimento, B.R., Neal, B., Neamati, N., Negoi, I., Negoi, R.I., Neupane, S., Newton, C.R.J., Ngunjiri, J.W., Nguyen, A.Q., Nguyen, G., Nguyen, Ha Thu, Nguyen, H.L.T., Nguyen, Huong Thanh, Nguyen, M., Nguyen, N.B., Nichols, E., Nie, J., Ningrum, D.N.A., Nirayo, Y.L., Nishi, N., Nixon, M.R., Nojomi, M., Nomura, S., Norheim, O.F., Noroozi, M., Norrving, B., Noubiap, J.J., Nouri, H.R., Shiadeh, M.N., Nowroozi, M.R., Nsoesie, E.O., Nyasulu, P.S., Obermeyer, C.M., Odell, C.M., Ofori-Asenso, R., Ogbo, F.A., Oh, I.H., Oladimeji, O., Olagunju, A.T., Olagunju, T.O., Olivares, P.R., Olsen, H.E., Olusanya, B.O., Olusanya, J.O., Ong, K.L., Ong, S.K., Oren, E., Orpana, H.M., Ortiz, A., Ota, E., Otstavnov, S.S., Overland, S., Owolabi, M.O., Mahesh, P., Pacella, R., Pakhare, A.P., Pakpour, A.H., Pana, A., Panda-Jonas, S., Park, E.K., Parry, C.D.H., Parsian, H., Patel, S., Pati, S., Patil, S.T., Patle, A., Patton, G.C., Paudel, D., Paulson, K.R., Ballesteros, W.C.P., Pearce, N., Pereira, A., Pereira, D.M., Perico, N., Pesudovs, K., Petzold, M., Pham, H.Q., Phillips, M.R., Pillay, J.D., Piradov, M.A., Pirsaheb, M., Pischon, T., Pishgar, F., Plana-Ripoll, O., Plass, D., Polinder, S., Polkinghorne, K.R., Postma, M.J., Poulton, R., Pourshams, A., Poustchi, H., Prabhakaran, D., Prakash, S., Prasad, N., Purcell, C.A., Purwar, M.B., Qorbani, M., Radfar, A., Rafay, A., Rafiei, A., Rahim, F., Rahimi, Z., Rahimi-Movaghar, A., Rahimi-Movaghar, V., Rahman, M., Rahman, M.H.U., Rahman, M.A., Rai, R.K., Rajati, F., Rajsic, S., Raju, S.B., Ram, U., Ranabhat, C.L., Ranjan, P., Rath, G.K., Rawaf, D.L., Rawaf, S., Reddy, K.S., Rehm, C.D., Rehm, J., Reiner, R.C., Reitsma, M.B., Remuzzi, G., Renzaho, A.M.N., Resnikoff, S., Reynales-Shigematsu, L.M., Rezaei, S., Ribeiro, A.L.P., Rivera, J.A., Roba, K.T., Rodríguez-Ramírez, S., Roever, L., Román, Y., Ronfani, L., Roshandel, G., Rostami, A., Roth, G.A., Rothenbacher, D., Roy, A., Rubagotti, E., Rushton, L., Sabanayagam, C., Sachdev, P.S., Saddik, B., Sadeghi, E., Moghaddam, S.S., Safari, H., Safari, Y., Safari-Faramani, R., Safdarian, M., Safi, S., Safiri, S., Sagar, R., Sahebkar, A., Sahraian, M.A., Sajadi, H.S., Salam, N., Salamati, P., Saleem, Z., Salimi, Y., Salimzadeh, H., Salomon, J.A., Salvi, D.D., Salz, I., Samy, A.M., Sanabria, J., Sanchez-Nino, M.D., Sánchez-Pimienta, T.G., Sanders, T., Sang, Y., Santomauro, D.F., Santos, I.S., Santos, J.V., Milicevic, M.M.S., Jose, B.P.S., Sardana, M., Sarker, A.R., Sarmiento-Suárez, R., Sarrafzadegan, N., Sartorius, B., Sarvi, S., Sathian, B., Satpathy, M., Sawant, A.R., Sawhney, M., Saylan, M., Sayyah, M., Schaeffner, E., Schmidt, M.I., Schneider, I.J.C., Schöttker, B., Schutte, A.E., Schwebel, D.C., Schwendicke, F., Scott, J.G., Seedat, S., Sekerija, M., Sepanlou, S.G., Serre, M.L., Serván-Mori, E., Seyedmousavi, S., Shabaninejad, H., Shaddick, G., Shafieesabet, A., Shahbazi, M., Shaheen, A.A., Shaikh, M.A., Levy, T.S., Shams-Beyranvand, M., Shamsi, M., Sharafi, H., Sharafi, K., Sharif, M., Sharif-Alhoseini, M., Sharifi, H., Sharma, J., Sharma, M., Sharma, R., She, J., Sheikh, A., Shi, P., Shibuya, K., Shiferaw, M.S., Shigematsu, M., Shin, M.J., Shiri, R., Shirkoohi, R., Shiue, I., Shokraneh, F., Shoman, H., Shrime, M.G., Shupler, M.S., Si, S., Siabani, S., Sibai, A.M., Siddiqi, T.J., Sigfusdottir, I.D., Sigurvinsdottir, R., Silva, D.A.S., Silva, J.P., Silveira, D.G.A., Singh, J.A., Singh, N.P., Singh, V., Sinha, D.N., Skiadaresi, E., Skirbekk, V., Smith, D.L., Smith, M., Sobaih, B.H., Sobhani, S., Somayaji, R., Soofi, M., Sorensen, R.J.D., Soriano, J.B., Soyiri, I.N., Spinelli, A., Sposato, L.A., Sreeramareddy, C.T., Srinivasan, V., Starodubov, V.I., Steckling, N., Stein, D.J., Stein, M.B., Stevanovic, G., Stockfelt, L., Stokes, M.A., Sturua, L., Subart, M.L., Sudaryanto, A., Sufiyan, M.B., Sulo, G., Sunguya, B.F., Sur, P.J., Sykes, B.L., Szoeke, C.E.I., Tabarés-Seisdedos, R., Tabuchi, T., Tadakamadla, S.K., Takahashi, K., Tandon, N., Tassew, S.G., Tavakkoli, M., Taveira, N., Tehrani-Banihashemi, A., Tekalign, T.G., Tekelemedhin, S.W., Tekle, M.G., Temesgen, H., Temsah, M.H., Temsah, O., Terkawi, A.S., Tessema, B., Teweldemedhin, M., Thankappan, K.R., Theis, A., Thirunavukkarasu, S., Thomas, H.J., Thomas, M.L., Thomas, N., Thurston, G.D., Tilahun, B., Tillmann, T., To, Q.G., Tobollik, M., Tonelli, M., Topor-Madry, R., Torre, A.E., Tortajada-Girbés, M., Touvier, M., Tovani-Palone, M.R., Towbin, J.A., Tran, B.X., Tran, K.B., Truelsen, T.C., Truong, N.T., Tsadik, A.G., Car, L.T., Tuzcu, E.M., Tymeson, H.D., Tyrovolas, S., Ukwaja, K.N., Ullah, I., Updike, R.L., Usman, M.S., Uthman, O.A., Vaduganathan, M., Vaezi, A., Valdez, P.R., Van Donkelaar, A., Varavikova, E., Varughese, S., Vasankari, T.J., Venkateswaran, V., Venketasubramanian, N., Villafaina, S., Violante, F.S., Vladimirov, S.K., Vlassov, V., Vollset, S.E., Vos, T., Vosoughi, K., Vu, G.T., Vujcic, I.S., Wagnew, F.S., Waheed, Y., Waller, S.G., Walson, J.L., Wang, Yafeng, Wang, Yanping, Wang, Y.P., Weiderpass, E., Weintraub, R.G., Weldegebreal, F., Werdecker, A., Werkneh, A.A., West, J.J., Westerman, R., Whiteford, H.A., Widecka, J., Wijeratne, T., Winkler, A.S., Wiyeh, A.B., Wiysonge, C.S., Wolfe, C.D.A., Wong, T.Y., Wu, S., Xavier, D., Xu, G., Yadgir, S., Yadollahpour, A., Jabbari, S.H.Y., Yamada, T., Yan, L.L., Yano, Y., Yaseri, M., Yasin, Y.J., Yeshaneh, A., Yimer, E.M., Yip, P., Yisma, E., Yonemoto, N., Yoon, S.J., Yotebieng, M., Younis, M.Z., Yousefifard, M., Yu, C., Zaidi, Z., Zaman, S. Bin, Zamani, M., Zavala-Arciniega, L., Zhang, A.L., Zhang, H., Zhang, K., Zhou, M., Zimsen, S.R.M., Zodpey, S., Murray, C.J.L., 2018. Global, regional, and national comparative risk assessment of 84 behavioural, environmental and occupational, and metabolic risks or clusters of risks for 195 countries and territories, 1990-2017: a systematic analysis for the Global Burden of Disease Study 2017. Lancet 392, 1923–1994. https://doi.org/10.1016/S0140-6736(18)32225-6.

Stenner, R.D., 1977a. The concentration of some heavy metals in sediments in some Mendip caves, and an assessment of the significance of un-natural contamination. Proc. Seventh Int. Speleol. Congr. Sheff, pp. 383–384.

Stenner, R.D., 1977b. The natural removal of some heavy metals from streams by limestone. Proc. Seventh Int. Speleol. Congr. Sheff, pp. 384–387.

Stenner, R.D., 1978. The concentration of cadmium, copper, lead and zinc in sediments from some caves and associated surface streams on Mendip, Somerset. Br. Cave Res. Assoc. Trans. 5, 113–120.

Stenner, R.D., 1979. The concentration of copper, lead and zinc in sediments in Wookey Hole cave, Somerset. Proc. Univ. Bristol Spelæological Soc. 15, 49–52.

Stenner, R.D., 1997. Changes in the distribution of water between surface sinks and stream inlets between surface sinks and stream inlets in St. Cuthbert's Swallet, Priddy, Somerset. Proc. Univ. Bristol Spelæological Soc. 21, 9–24.

Microbial life of cave systems. In: Summers Engel, A. (Ed.), Microbial Life of Cave Systems. DE GRUYTER, Berlin, München, Boston https://doi.org/10.1515/9783110339888.

Taylor, D.L., Walters, W.A., Lennon, N.J., Bochicchio, J., Krohn, A., Caporaso, J.G., Pennanen, T., 2016. Accurate estimation of fungal diversity and abundance through improved lineage-specific primers optimized for Illumina amplicon sequencing. Appl. Environ. Microbiol. 82, 7217–7226. https://doi.org/10.1128/AEM.02576-16.

Tebo, B.M., 1991. Manganese(II) oxidation in the suboxic zone of the Black Sea. Deep. Res. Part A 38, S883–S905. https://doi.org/10.1016/s0198-0149(10)80015-9.

Tebo, B.M., Bargar, J.R., Clement, B.G., Dick, G.J., Murray, K.J., Parker, D., Verity, R., Webb, S.M., 2004. Biogenic manganese oxides: properties and mechanisms of formation. Annu. Rev. Earth Planet. Sci. 32, 287–328. https://doi.org/10.1146/annurev.earth.32.101802.120213.

Tebo, B.M., Johnson, H.A., McCarthy, J.K., Templeton, A.S., 2005. Geomicrobiology of manganese(II) oxidation. Trends Microbiol. 13, 421–428. https://doi.org/10.1016/j.tim.2005.07.009.

Tebo, B.M., Clement, B.G., Dick, G.J., 2014. Biotransformations of manganese. Manual of Environmental Microbiology, Third edition American Society of Microbiology, pp. 1223–1238 https://doi.org/10.1128/9781555815882.ch100.

Timonin, M., 1950. Soil microflora in relation to manganese deficiency. Sci. Agric. 30, 324–325. https://doi.org/10.4141/sa-1950-0039.

Tonkin, J.W., Balistrieri, L.S., Murray, J.W., 2004. Modeling sorption of divalent metal cations on hydrous manganese oxide using the diffuse double layer model. Appl. Geochem. 19, 29–53. https://doi.org/10.1016/S0883-2927(03)00115-X.

Van Der Heggen, M., Martins, S., Flores, G., Soares, E.V., 2010. Lead toxicity in *Saccharomyces cerevisiae*. Appl. Microbiol. Biotechnol. 88, 1355–1361. https://doi.org/10.1007/s00253-010-2799-5.

Villalobos, M., Toner, B., Bargar, J., Sposito, G., 2003. Characterization of the manganese oxide produced by *Pseudomonas putida* strain MnB1. Geochim. Cosmochim. Acta 67, 2649–2662. https://doi.org/10.1016/S0016-7037(03)00217-5.

Villalobos, M., Bargar, J., Sposito, G., 2005. Mechanisms of Pb(II) sorption on a biogenic manganese oxide. Environ. Sci. Technol. 39, 569–576. https://doi.org/10.1021/es049434a.

Waltham, A.C., Simms, M.J., Farrant, A.R., Goldie, H.S. (Eds.), 1997. Karst and Caves of Great Britain (Geological Conservation Review Series). Chapman & Hall.

Wang, Z., Giammar, D.E., 2013. Mass action expressions for bidentate adsorption in surface complexation modeling: theory and practice. Environ. Sci. Technol. 47, 3982–3996. https://doi.org/10.1021/es305180e.

Webb, S.M., Dick, G.J., Bargar, J.R., Tebo, B.M., 2005. Evidence for the presence of Mn(III) intermediates in the bacterial oxidation of Mn(II). Proc. Natl. Acad. Sci. U. S. A. 102, 5558–5563. https://doi.org/10.1073/pnas.0409119102.

White, W.B., Vito, C., Scheetz, B.E., 2009. The mineralogy and trace element chemistry of black manganese oxide deposits from caves. J. Cave Karst Stud. 71, 136–143.

Willems, A., 2014. The family *Phyllobacteriaceae*. The Prokaryotes: Alphaproteobacteria and Betaproteobacteria. Springer-Verlag, Berlin Heidelberg, pp. 355–418 https://doi.org/10.1007/978-3-642-30197-1_298.

World Health Organisation, 2010. Childhood Lead Poisoning. WHO. World Health Organization, Geneva.

Yu, H., Leadbetter, J.R., 2020. Bacterial chemolithoautotrophy via manganese oxidation. Nature 583, 453–458. https://doi.org/10.1038/s41586-020-2468-5.

Zanardini, E., Andreoni, V., Borin, S., Cappitelli, F., Daffonchio, D., Talotta, P., Sorlini, C., Ranalli, G., Bruni, S., Cariati, F., 1997. Lead-resistant microorganisms from red stains of marble of the Certosa of Pavia, Italy and use of nucleic acid-based techniques for their detection. Int. Biodeterior. Biodegradation 40, 171–182. https://doi.org/10.1016/S0964-8305(97)00057-7.

Zappelini, C., Alvarez-Lopez, V., Capelli, N., Guyeux, C., Chalot, M., 2018. *Streptomyces* dominate the soil under betula trees that have naturally colonized a red gypsum landfill. Front. Microbiol. 9, 1772. https://doi.org/10.3389/fmicb.2018.01772.

Zeller, T., Klug, G., 2006. Thioredoxins in bacteria: functions in oxidative stress response and regulation of thioredoxin genes. Naturwissenschaften https://doi.org/10.1007/s00114-006-0106-1.

Zhu, H.Z., Zhang, Z.F., Zhou, N., Jiang, C.Y., Wang, B.J., Cai, L., Liu, S.J., 2019. Diversity, distribution and co-occurrence patterns of bacterial communities in a karst cave system. Front. Microbiol. 10, 1726. https://doi.org/10.3389/fmicb.2019.01726.

Złoch, M., Thiem, D., Gadzała-Kopciuch, R., Hrynkiewicz, K., 2016. Synthesis of siderophores by plant-associated metallotolerant bacteria under exposure to Cd^{2+}. Chemosphere 156, 312–325. https://doi.org/10.1016/j.chemosphere.2016.04.130.